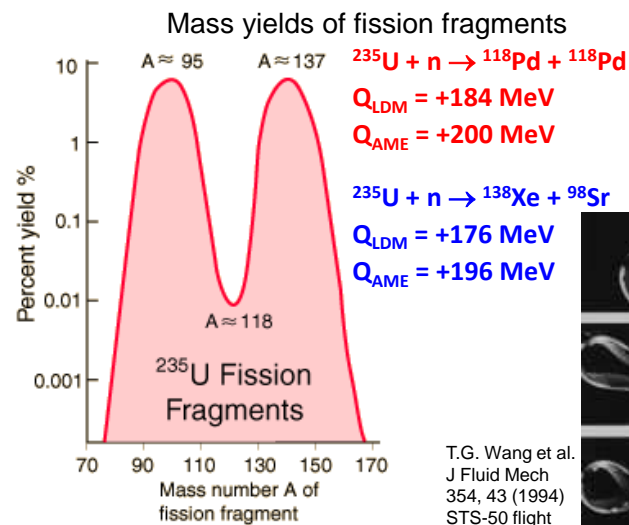


Interesting effects in well-known reactions and decays

Ulli Köster
Institut Laue-Langevin, Grenoble
and Chair GIE, Université Grenoble Alpes



École Joliot Curie
27/28 September 2017



Thomson 1910: parabola mass spectrograph

Electric field parallel to magnetic field

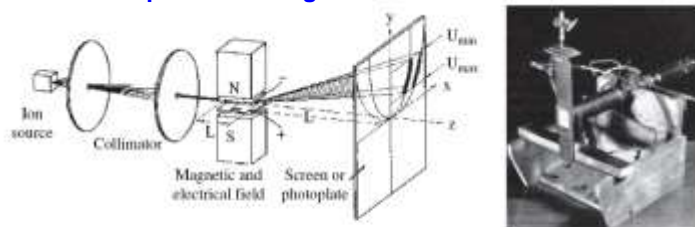
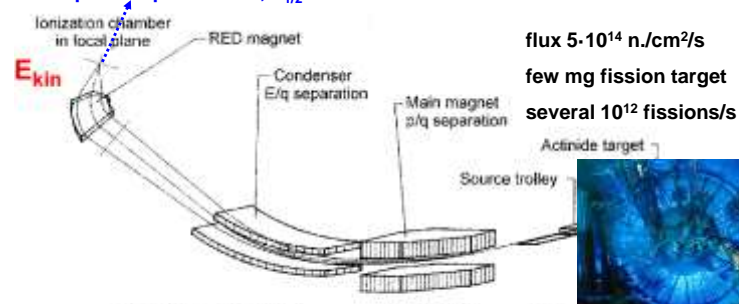


Figure 1.5 Parabola mass spectrograph constructed by J.J. Thomson (1910) with a discharge tube as ion source, a superimposed electrical field and a magnetic field oriented parallel to it for ion separation, and a photoplate for ion detection. (H. Kienitz (ed.), Massenspektrometrie (1968), Verlag Chemie, Weinheim. Reproduced by permission of Wiley-VCH.)

1912: Neon consists of two isotopes with mass 20 and 22

The LOHENGRIN fission fragment separator

mass-separated fission fragments, $\Delta A/A = 3\text{E-}4 - 3\text{E-}3$
 up to 10^5 per second, $T_{1/2} \geq \text{microsec.}$ $\Delta E/E = 1\text{E-}3 - 1\text{E-}2$



$$m v^2 / r_{\text{el}} = q E \quad m v^2 / r_{\text{magn}} = q v B$$

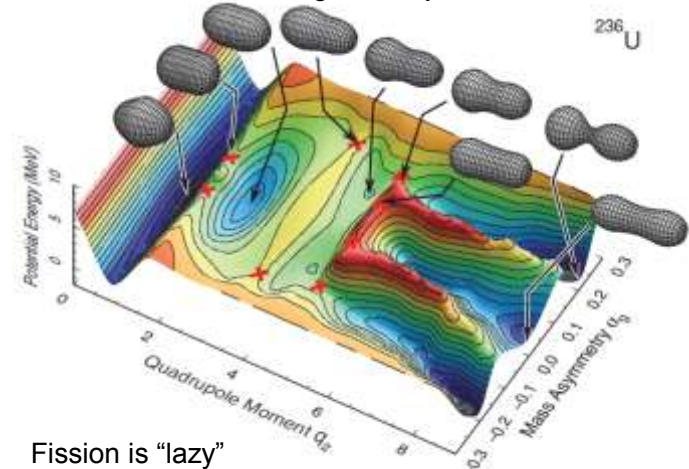
$$E_{\text{kin}} / q = E / 2 r_{\text{el}} \quad m v / q = B r_{\text{magn}}$$

P. Armbruster et al., Nucl. Instr. Meth. 139 (1976) 213.

The LOHENGRIN fission fragment spectrometer



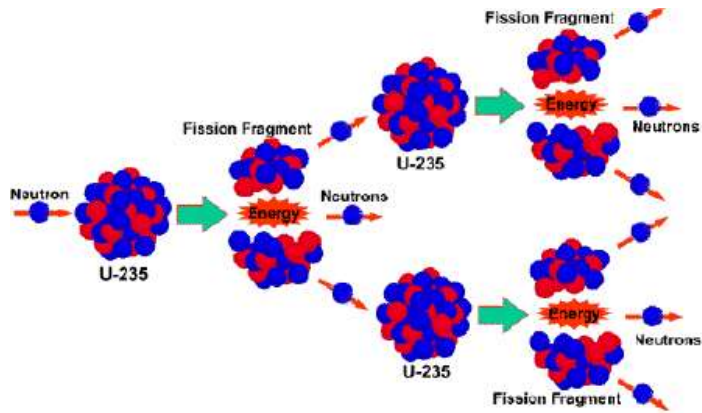
Understanding fission yields of ^{236}U



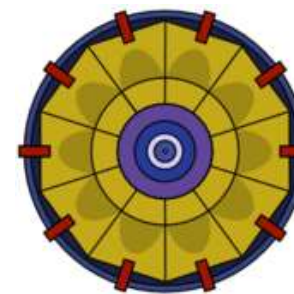
Fission is "lazy"

T. Ichikawa et al. PRC 86, 024610 (2012)

A nuclear chain reaction

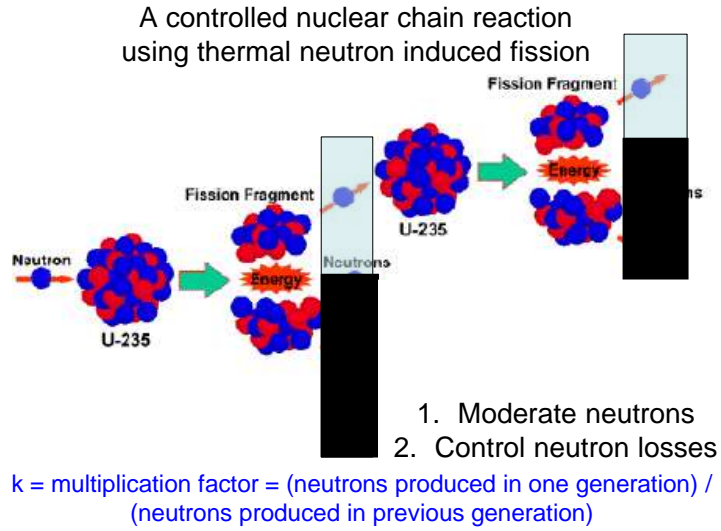
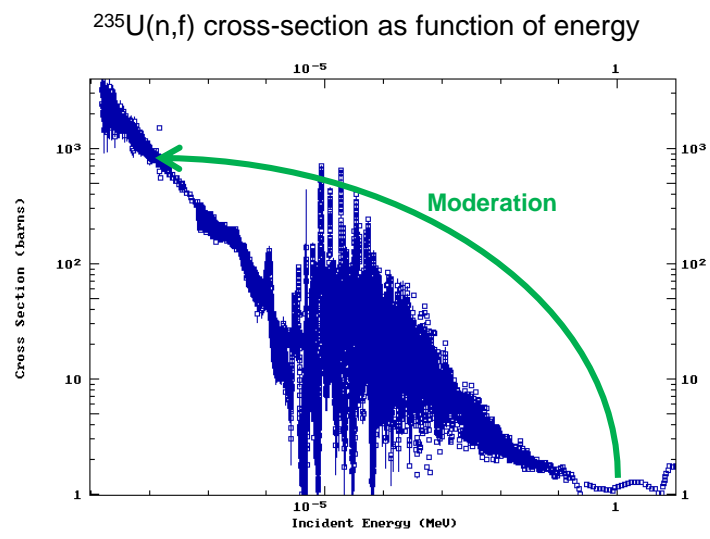


A single-pulse neutron source



Uncontrolled chain reaction of fast-neutron induced fission
 ≈ 25 kg of 93% ^{235}U





Prompt neutron kinetics

Prompt neutron lifetime τ_p is the average time between the birth of prompt fission neutrons and their final absorption.

Assumptions:

- No delayed neutrons
- Infinite reactor, multiplication factor $k_{\infty} = k$

time	N(t)
0	n
τ_p	kn
$2\tau_p$	k^2n
$3\tau_p$	k^3n

$$\frac{dn}{dt} = \frac{k-1}{\tau_p} n \Rightarrow n(t) = n(0)e^{\frac{(k-1)t}{\tau_p}}$$

Time constant $T = \frac{\tau_p}{k-1}$

Exponential decrease ($k < 1$) or exponential growth ($k > 1$)

cf. demographic projections for Germany
 Fertility: 1.5 child/women $\rightarrow k=0.75$
 $T = 25 \text{ years} / (1-0.75) = 100 \text{ years}$

Prompt neutron kinetics

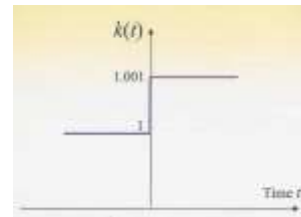
$\tau_p = \tau_s + \tau_d = \text{slowing down time} + \text{diffusion time}$

In thermal reactors: $\tau_s \ll \tau_d$, i.e. $\tau_p \cong \tau_d$

$\tau_d \cong \lambda_a/v \cong 10 \text{ cm} / (2000\text{m/s})$

$\tau_p \cong \tau_d \cong 50 \mu\text{sec}$

Example: step of reactivity from $k=1.000$ to $k=1.001$



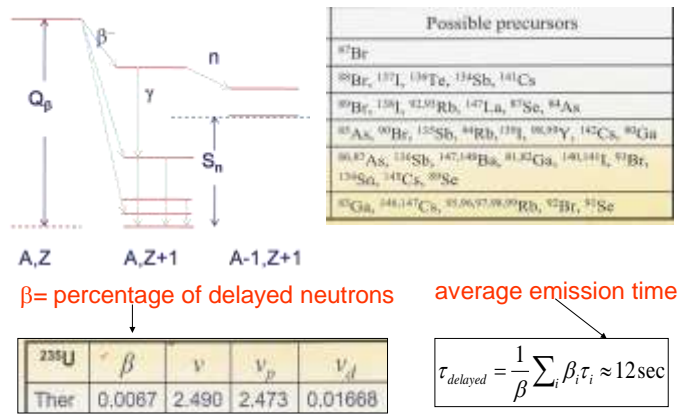
$T = \frac{\tau_p}{k-1} = \frac{50 \cdot 10^{-6}}{10^{-3}} = 0.05 \text{ sec}$

$n(t) = n_0 e^{\frac{t}{0.05}}$

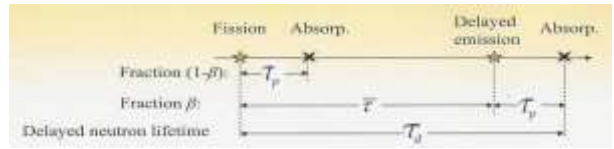
$\frac{n(1 \text{ sec})}{n_0} = e^{20} = 5E8$

“Prompt” control is not possible!

Delayed neutron emission from fission products



Neutron lifetime, taking into account delayed neutrons



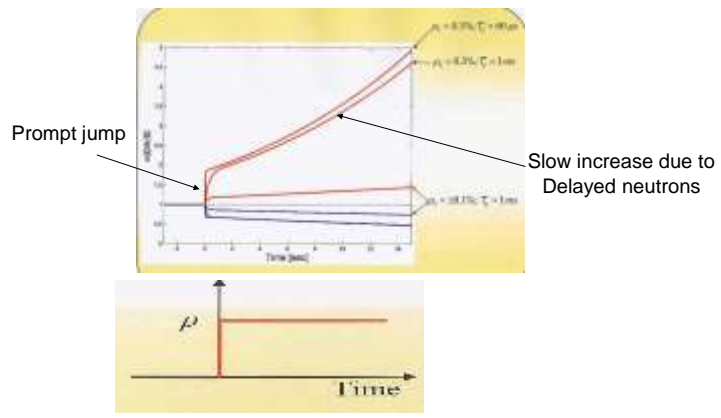
$$k = k_{\text{prompt}} + k_{\text{delayed}} = 1 = (1 - \beta) + \beta$$

$$\tau = (1 - \beta)\tau_p + \beta(\tau_{\text{delayed}} + \tau_p) \approx \beta\tau_{\text{delayed}} = 0.08 \text{ sec}$$

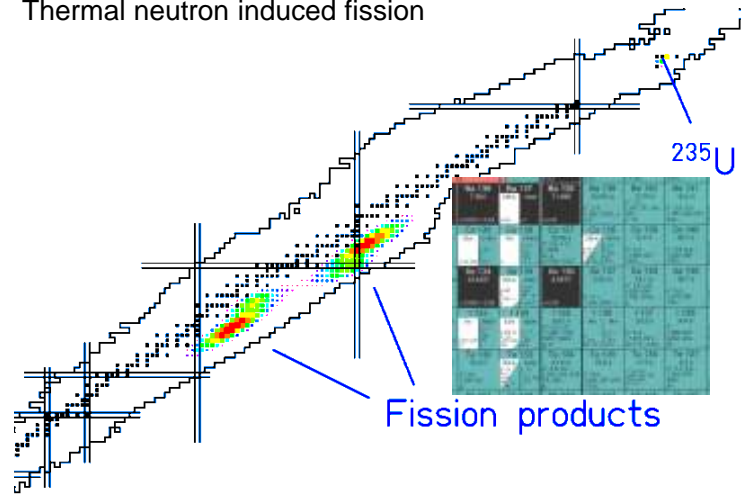
Now for step from k=1.000 to k=1.001

$$T = \beta\tau_{\text{delayed}} / (k-1) = 80 \text{ seconds}$$

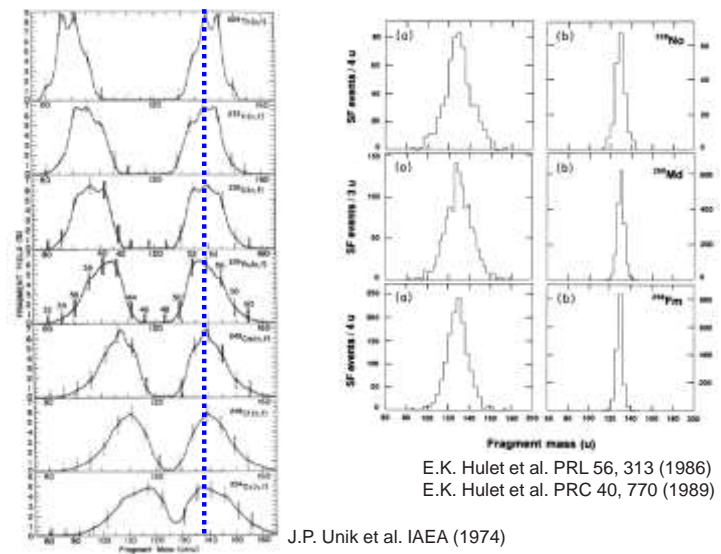
Reactor response to a step of reactivity



Thermal neutron induced fission



Interesting effects in well-known reactions and decays

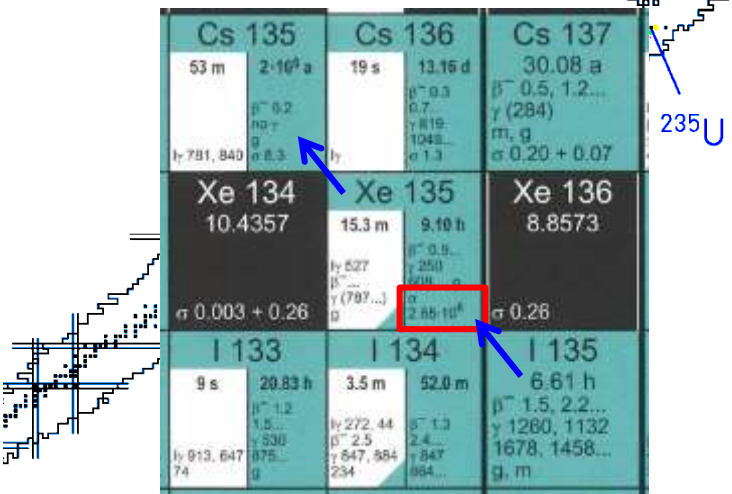


Delayed neutron yields

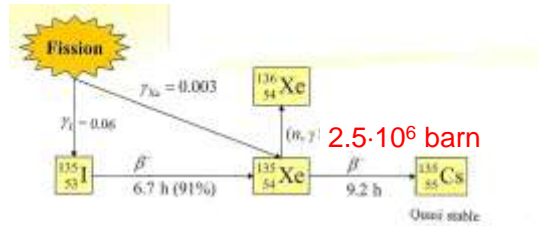
- $^{235}\text{U}(n_{th},f)$ 1.62%
- $^{239}\text{Pu}(n_{th},f)$ 0.63%
- $^{238}\text{U}(n_f,f)$ 4.39%
- $^{239}\text{Pu}(n_f,f)$ 0.63%

Isotope	F	Table 1-174	Waste	Inventory	1st	2nd	3rd	4th	5th	6th	7th	8th	9th	10th
U232	F	0.310(0.03)			4.01	3.1	0.018							
Pu231	T					1.60	1.60	1.60						
U232	F	3.110(1.1)				1.60	1.60	1.60						
U232	F		0.000(0.0)			0.00	0.00	0.00						
U233	T	0.0070(0.007)	0.140(0.0)		0.70	0.71	0.71	0.71						
U235	F	0.731(0.009)		0.779(0.04)	0.70	1.04	1.04	1.04						
U234	F	1.000(0.10)				1.01	1.01	1.01						
U238	T	1.627(0.009)	1.67(0.0)		1.69	1.69	1.69	1.69						
U236	F	1.073(0.009)			1.09	1.09	1.09	1.09						
U238	F	2.210(0.00)				2.19	2.19	2.19						
U237	T					2.30	2.30	2.30						
U237	F		4.00(0.2)		4.01	3.00	3.00	3.00						
U238	F				4.02	4.00	4.00	4.00						
U238	F	4.300(0.00)				4.30	4.30	4.30						
Np237	T		1.07(0.1)		1.00	1.00	1.00	1.00						
Np237	F			1.22(0.00)		1.10	1.10	1.10						
Np239	T				2.15	2.15	2.15	2.15						
Np239	F				2.11	2.10	2.10	2.10						
Pu238	T		0.48(0.07)		0.47	0.47	0.47	0.47						
Pu238	F	0.47(0.00)		0.49(0.00)	0.47	0.47	0.47	0.47						
Pu239	T	0.60(0.00)	0.60(0.0)		0.60	0.60	0.60	0.60						
Pu239	F	0.60(0.0)			0.60	0.60	0.60	0.60						
Pu240	T		0.90(0.0)		0.90	0.90	0.90	0.90						
Pu240	F	0.88(0.00)		0.91(0.00)	0.88	0.88	0.88	0.88						
Pu241	T	1.62(0.1)	1.67(0.1)		1.67	1.67	1.67	1.67						
Pu241	F	1.62(0.1)		1.66(0.0)	1.66	1.66	1.66	1.66						
Pu242	T		1.80(0.0)		1.80	1.80	1.80	1.80						
Pu242	F	2.21(0.00)			2.21	2.21	2.21	2.21						
Am241	T		0.44(0.0)		0.44	0.44	0.44	0.44						
Am241	F			0.39(0.00)	0.41	0.41	0.41	0.41						
Am242M	T		0.00(0.0)		0.00	0.00	0.00	0.00						
Am242M	F				0.00	0.00	0.00	0.00						
Am243	T				0.60	0.60	0.60	0.60						
Am243	F				0.60	0.60	0.60	0.60						
Cm245	T		0.90(0.0)		0.90	0.90	0.90	0.90						
Cm245	F				0.90	0.90	0.90	0.90						
Cm248	T		0.27(0.0)		0.28	0.28	0.28	0.28						
Cm248	F				0.28	0.28	0.28	0.28						
Cm251	T				0.73	0.73	0.73	0.73						

Thermal neutron induced fission



Reactor poisoning by ^{135}Xe



$$\frac{dN_i}{dt} = \gamma_i \sum_j \phi_{th} - \lambda_i N_i$$

$$N_i(t) = \frac{\gamma_i \sum_j \phi_{th}}{\lambda_i} (1 - e^{-\lambda_i t}) \rightarrow N_i^{eq} = \frac{\gamma_i \sum_j \phi_{th}}{\lambda_i}$$

$$\frac{dN_{Xe}}{dt} = \lambda_I N_I + Y_{Xe} \sum_j \phi - \lambda_{Xe} N_{Xe} - \sigma_c^{Xe} N_{Xe} \Phi \rightarrow N_{Xe}^{eq} = \frac{(Y_I + Y_{Xe}) \sum_j \phi}{\lambda_{Xe} + \sigma_c^{Xe} \Phi}$$

Xenon equilibrium concentration

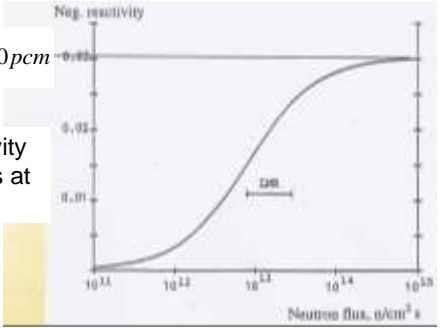
Reactivity due to Xe poisoning

$$\Delta\rho = -\frac{\Sigma_{\text{xenon}}}{\nu\Sigma_f} = -\frac{\sigma_X X}{\nu\Sigma_f} \longrightarrow \Delta\rho^{\text{xenon}} = -\frac{Y_T}{(\lambda_X + \sigma_X\Phi)} \frac{\Phi\sigma_X}{\nu}$$

High flux limit

$$\Delta\rho = -\frac{Y_T}{\nu} = -\frac{0.063}{2.45} \approx -2600 \text{ pcm}$$

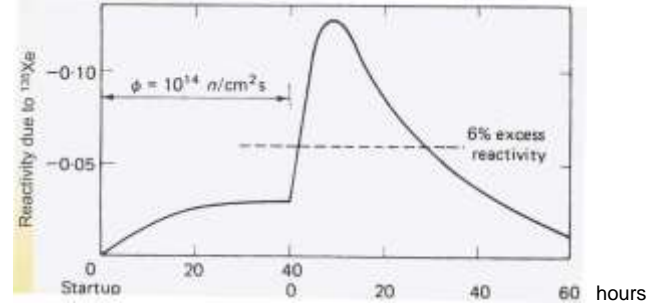
The maximum anti-reactivity is reached after 1 - 2 days at full power



Xenon transient following a shutdown

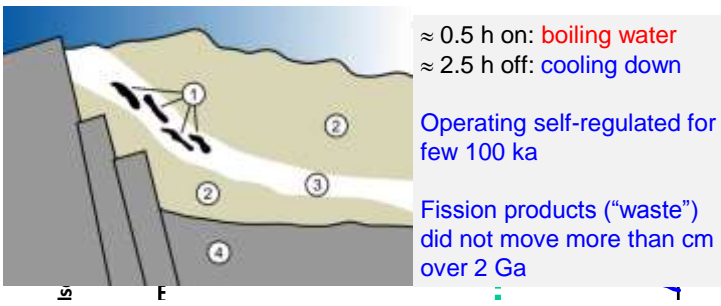
$$\frac{dN_{\text{Xe}}}{dt} = \lambda_I N_I + Y_{\text{Xe}} \Sigma_f \Phi - \lambda_{\text{Xe}} N_{\text{Xe}} - \sigma_c^{\text{Xe}} N_{\text{Xe}} \Phi$$

No more neutrons to destroy ¹³⁵Xe



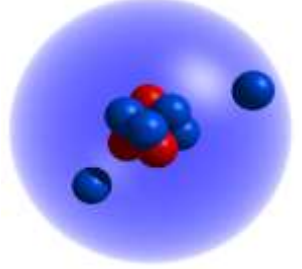
The anti reactivity increase prevents restarting of the reactor if a large enough positive reactivity reserve is not available!

The first nuclear reactor

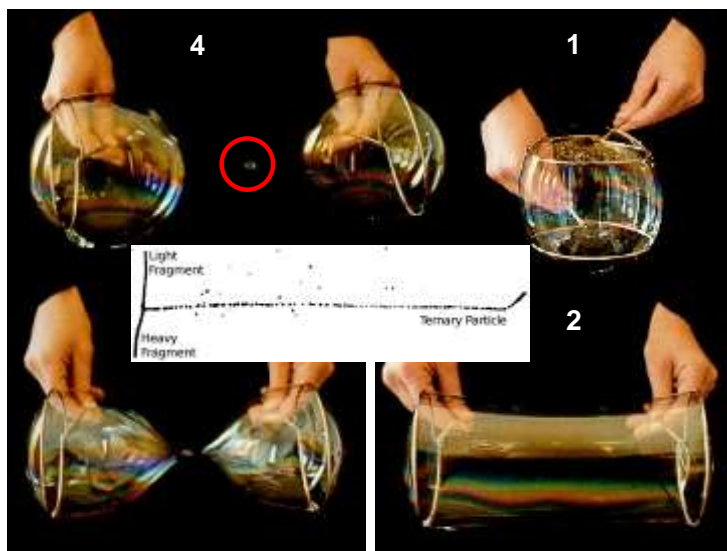


In nuclear reactors a **NEGATIVE FEEDBACK** is very **POSITIVE** (=good/useful)!

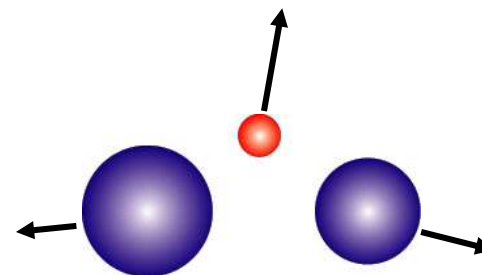
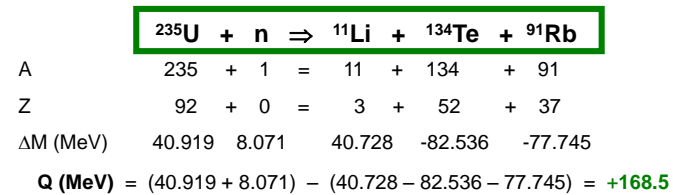
¹¹Li production in thermal neutron induced fission?



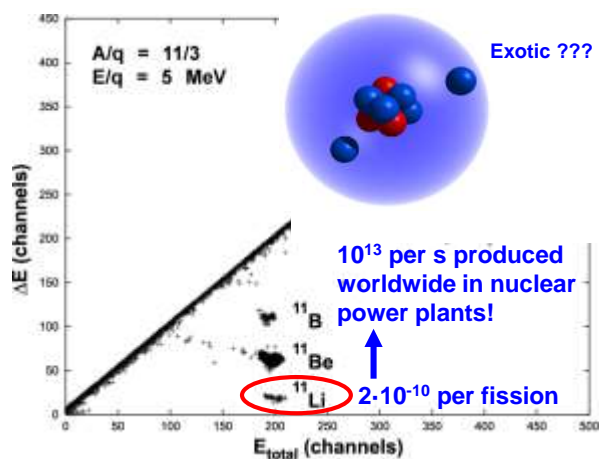
A	235	+	1	=	11	+	225
Z	92	+	0	=	3	+	89
ΔM (MeV)	40.919		8.071		40.728		21.639
Q (MeV)	= (40.919 + 8.071) - (40.728 + 21.639) = -13.4						



^{11}Li production in thermal neutron induced fission?



Detection of rare ternary particles



Nucl. Phys. A652, 371.

cea
Context

Ternary particles: important source tritium production in nuclear reactors and in used fuel elements

Following the various processing campaigns of French and foreign spent fuel assemblies, AREVA has observed several singular behaviors :

- The quantity of tritium released into the sea from EDF spent fuel assemblies is higher than from foreign one;
- A quantity of liquid tritium from EDF 1300 MWe spent fuel assemblies is greater than from EDF 900 MWe;
- By extrapolation, the maximum limit "tritium" activity authorized by French 'Autorité de Sureté Nucléaire' could be reached in 2015-2020.

Nuclear Data concerning the tritium production are requested

O. Serot. JEFF 2014.

cea Context

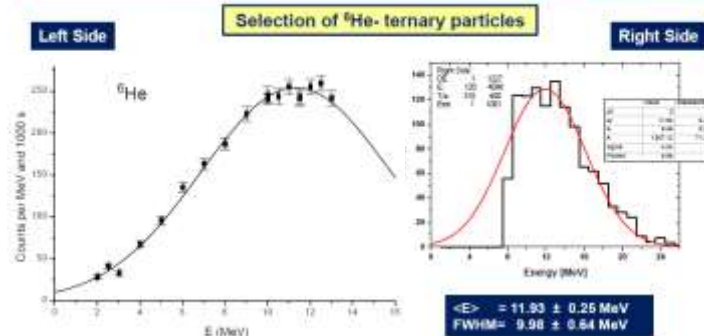
Calculations performed for UOx (3.25%) at 33GWd/t (J. Pavageau, private communication)

Tritium Formation in UOx fuel element	Contribution
Direct production from Ternary Fission	81.94 %
Indirect Production from ⁶ He Ternary Fission:	
• ⁶ He → ⁴ Li + β	11.50 %
• ⁶ Li + n → ⁴ He + ² H (σ=941.3b)	
Indirect ³ H production	4.82 %
• ² H → ³ He + β	
• ³ He + n → p + ³ H (σ=5317b)	
Reaction (n, ² H) on ¹⁶ O:	0.96 %
n + ¹⁶ O → ¹⁴ N + ² H	
Reaction (n, ³ He) on ¹⁶ O:	0.05 %
• n + ¹⁶ O → ¹⁴ C + ² He	
• ² He + n → p + ³ H	

The accuracy of the tritium production could be improved by improving our knowledge on ⁶He ternary fission yields

O. Serot. JEFF 2014.

cea Measurement of ternary fission yields from ²⁴¹Pu(n_{th},f) reaction



⁶He ternary fission yield for ²⁴¹Pu(n,f): $(4.48 \pm 0.30) \times 10^{-5}$

O. Serot. JEFF 2014.

Ternary fission models



Double neck rupture model (Rubchenya and Yavshits)



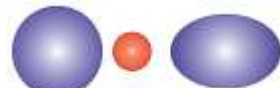
Boltzmann model (Faust and Bao)



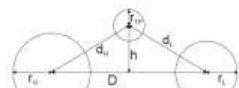
Modified double neck rupture model (Baum et al.)



Modified Halpern model (Gönnenwein and Wöstheinrich)

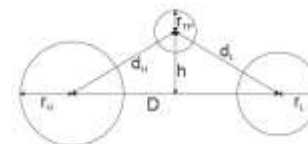


Transition energy model (Pik-Pichak)



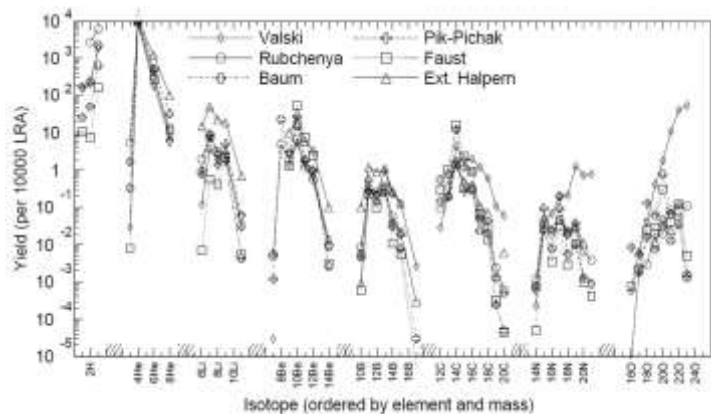
Universal parameterization

Ternary fission models

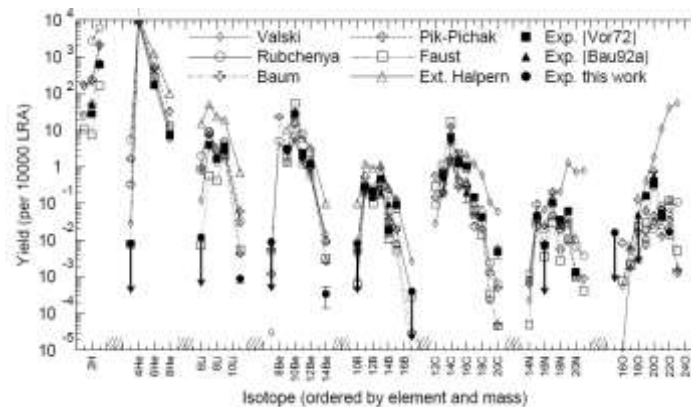


Model (ref.)	(A _H , Z _H)	(A _L , Z _L)	D fm	d _L fm	d _H fm	h fm	T MeV
[Rub88]	¹⁴⁰ Cs	⁸⁶ As ⁽¹¹⁾	≈ 25	11.2	≈ 13.8	0	2.1
[Rub94, Rubch]	¹³² Sn	⁹⁴ Sr	23.6	11.3	12.3	0	2.19
[Bau92b]	¹³² Sn	⁹⁴ Sr	22.6	13.6	14.2	7.5	1.91
[PP94]	¹³² Sn	⁹⁴ Sr	22.9	12.8	10.1	0	2.1 ⁽¹²⁾
[Fau95b]	¹³² Sn	⁹⁴ Sr	13.4	9.9	10.5	7.7	1.3
[Wös96]	¹³² Sn ⁽¹³⁾	⁹⁴ Sr	22.4	10.8	11.6	0	(3.1) ⁽¹⁴⁾

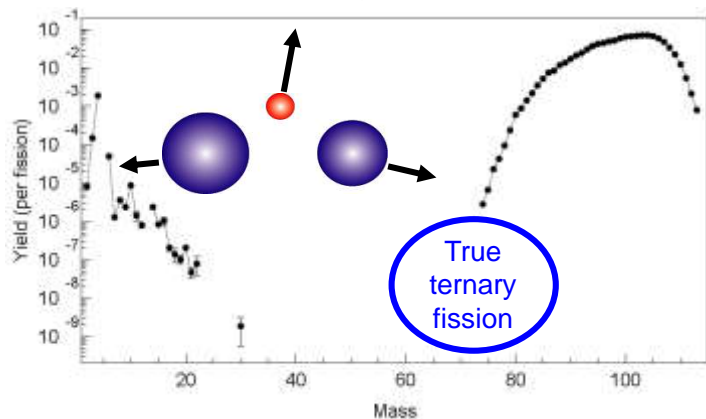
Ternary fission models



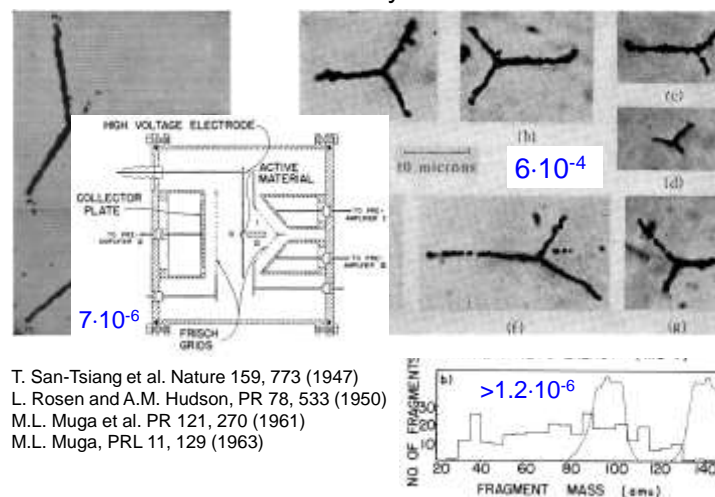
Comparison with measurement



Ternary fission

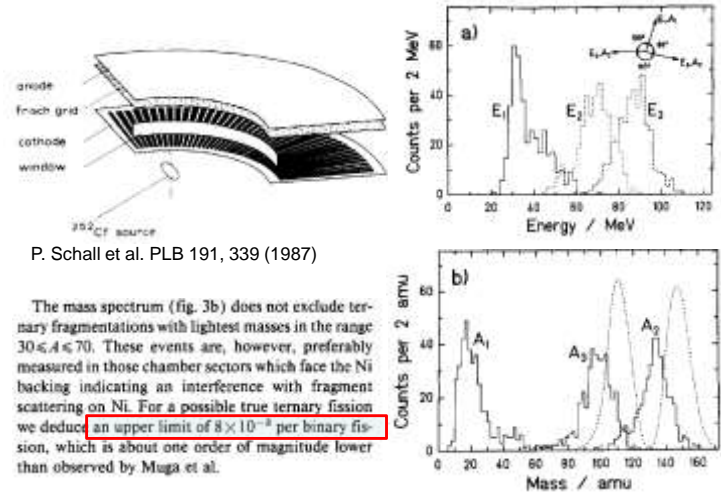


"True ternary fission"

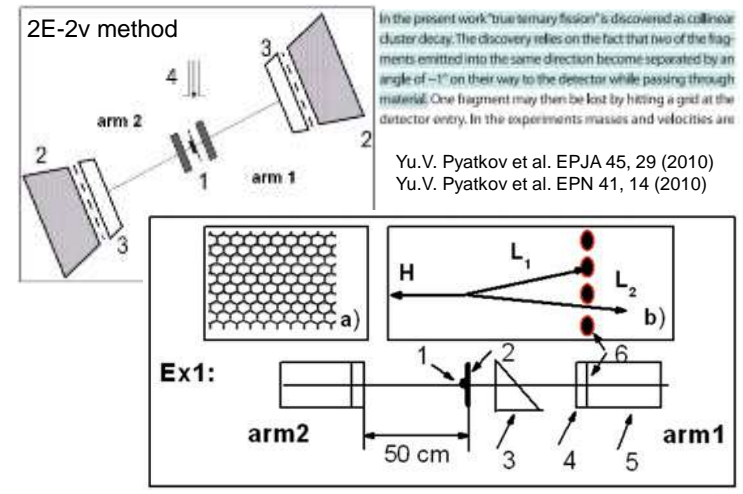


T. San-Tsiang et al. Nature 159, 773 (1947)
 L. Rosen and A.M. Hudson, PR 78, 533 (1950)
 M.L. Muga et al. PR 121, 270 (1961)
 M.L. Muga, PRL 11, 129 (1963)

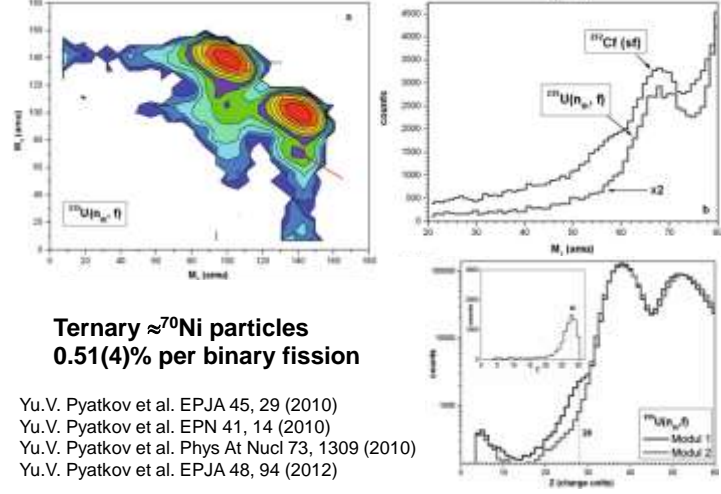
DIOGENES: upper limit for true ternary fission



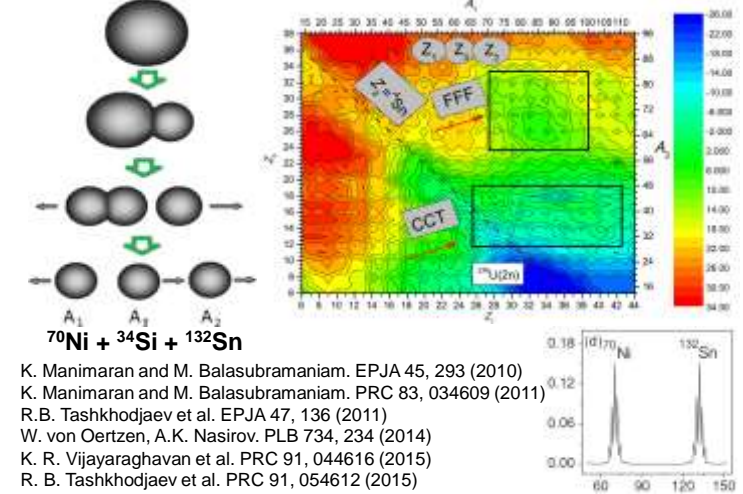
FOBOS



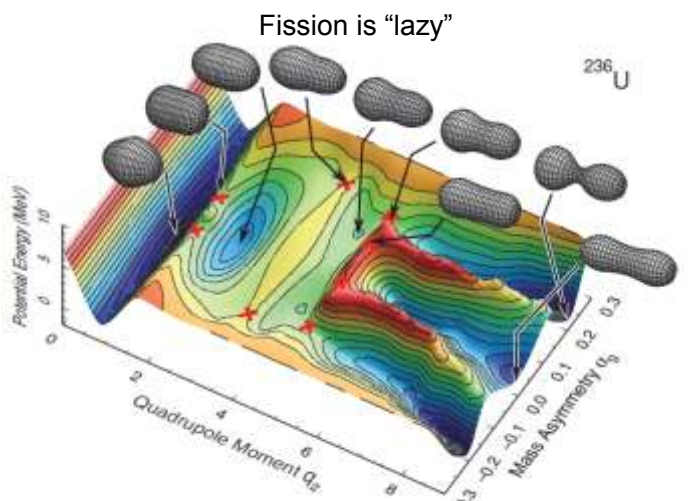
FOBOS finds Collinear Cluster Tripartition (CCT)



Collinear Cluster Tripartition (CCT)

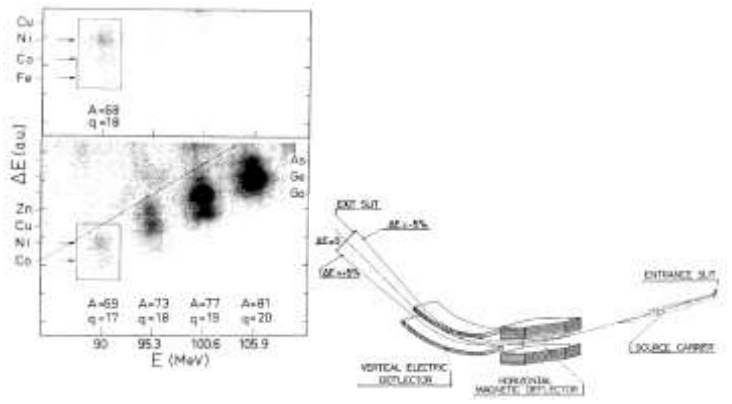


Interesting effects in well-known reactions and decays



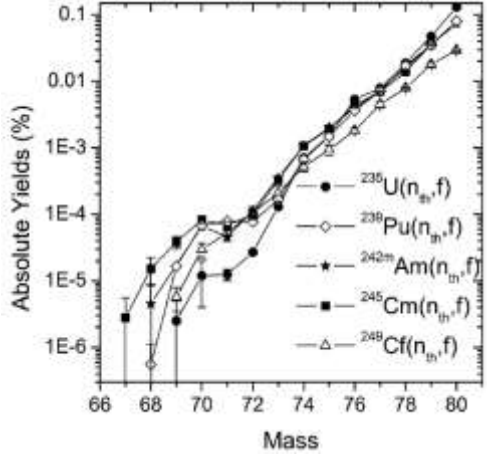
T. Ichikawa et al. PRC 86, 024610 (2012)

Discovery of ⁶⁸Fe and ^{68,69}Co



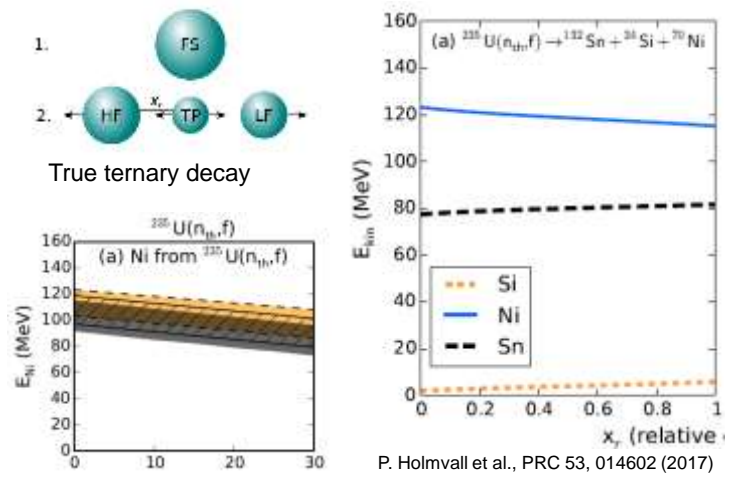
M. Bernas et al. PRL 67, 3661 (1991)

Far asymmetric fission studied at LOHENGRIN



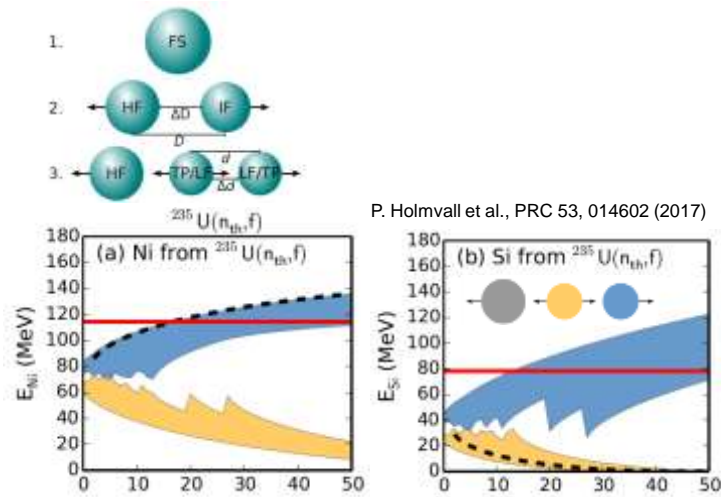
D. Rochman et al. NPA 735, 3 (2004)

Calculation of allowed kinetic energy range

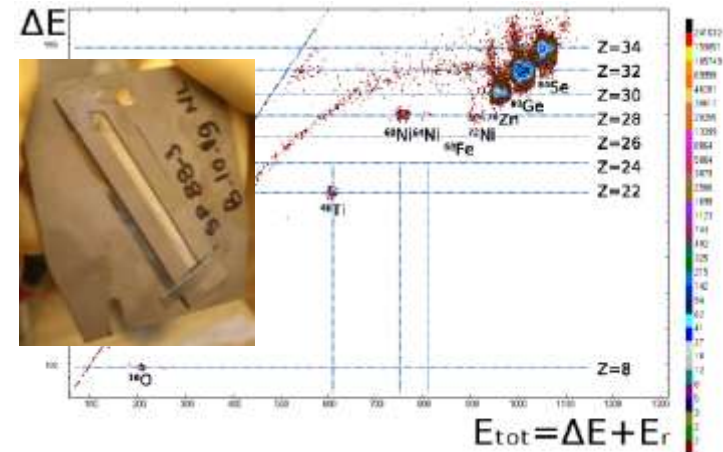


P. Holmval et al., PRC 53, 014602 (2017)

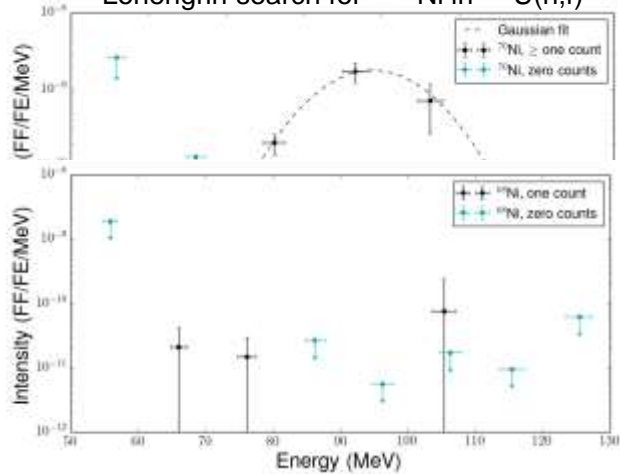
Allowed kinetic energies in sequential model



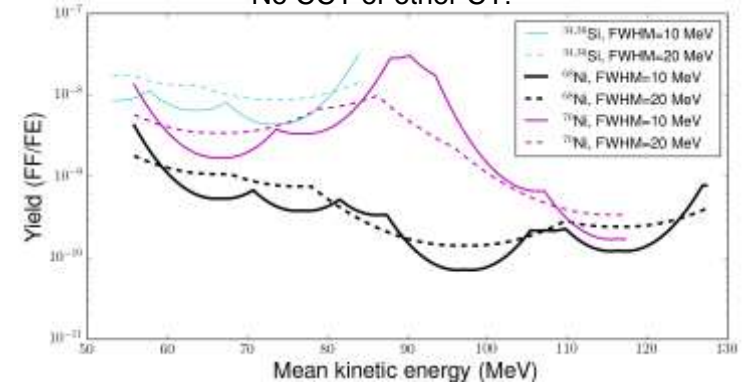
$\Delta E/E$ identification plot: $A/q = 4$



Lohengrin search for $^{68,70}\text{Ni}$ in $^{235}\text{U}(n,f)$

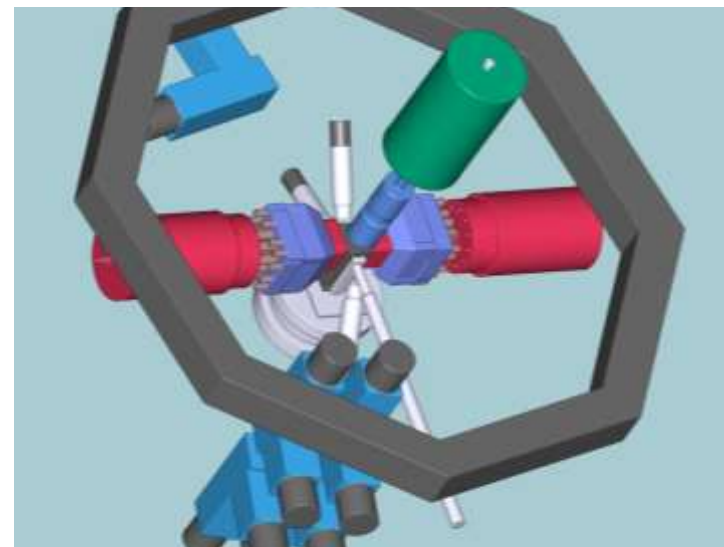
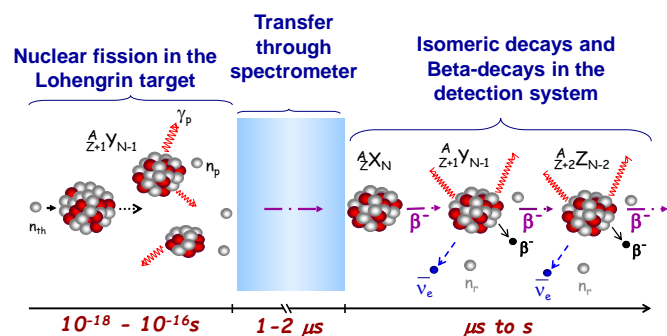


No CCT or other CT!

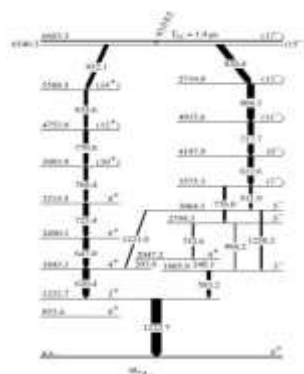
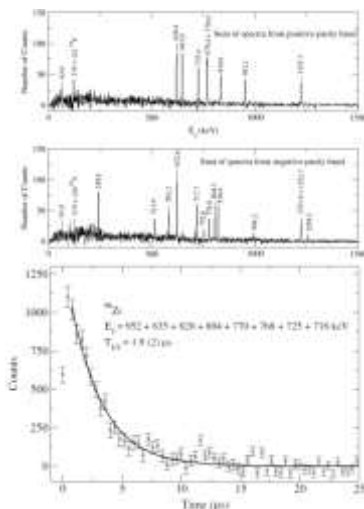


Cluster tripartition into $^{68,70}\text{Ni}$ refuted at 10^{-8} level

Fission product spectroscopy



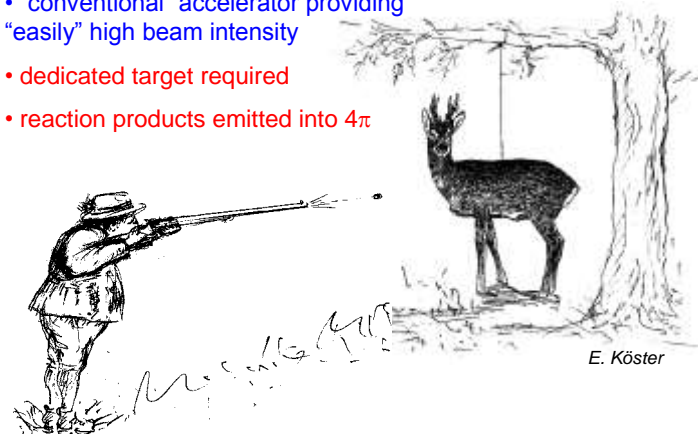
17- isomer at 6.6 MeV in ${}^{98}Zr$



Over 70 microsecond isomers studied so far at LOHENGRIN: $T_{1/2} \geq 0.5 \mu s$

Normal kinematics: n, p or light ions on heavy target

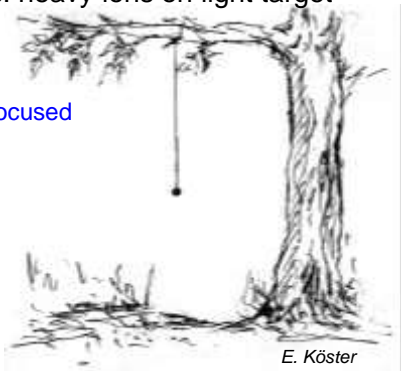
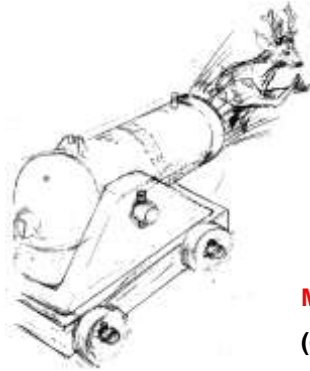
- “conventional” accelerator providing “easily” high beam intensity
- dedicated target required
- reaction products emitted into 4π



E. Köster

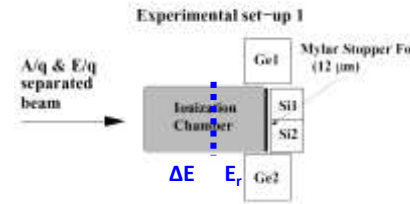
Inverse kinematics: heavy ions on light target

- complex and expensive accelerator
- reaction products forward focused



Mind the losses during stopping!
(graphical representation censored)

Detection setup



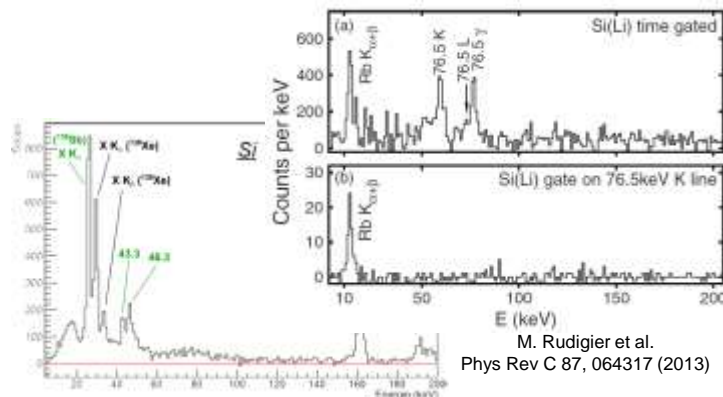
Gamma ray detection
Conversion-electron detection

Z identification via energy loss
(Bethe Bloch)

$$\frac{dE}{dx} \sim \frac{Z^2}{E}$$

Intrinsic advantage:
< 1 μm longitudinal straggling
cf. BigRIPS 1100 μm, FRS 4000 μm

Conversion electron spectroscopy at LOHENGRIN



$T_{1/2} > 500$ ns, $E > 12$ keV

G. Gey, PhD LPSC Grenoble (2014)

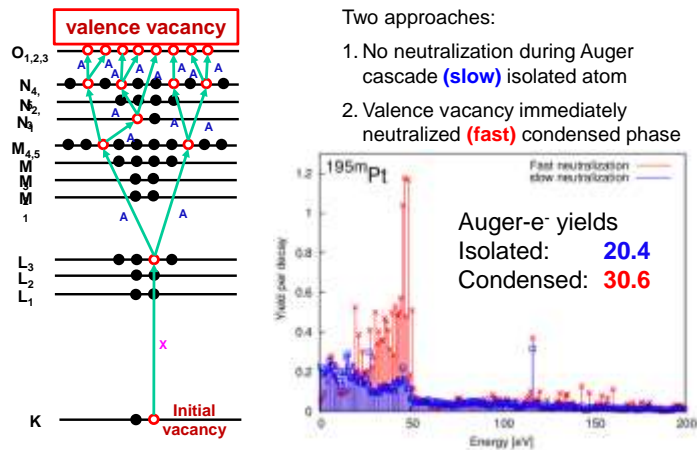
Which nuclear data do we need for nuclear medicine?

1. Half-life
2. Gamma ray energies (roughly!)
3. Particle spectra (electrons, alpha)

Lu 177
6.7 d
 β^- 0.5...
 γ 208, 113...



BrlccEmis: Simulation of Auger electron spectra



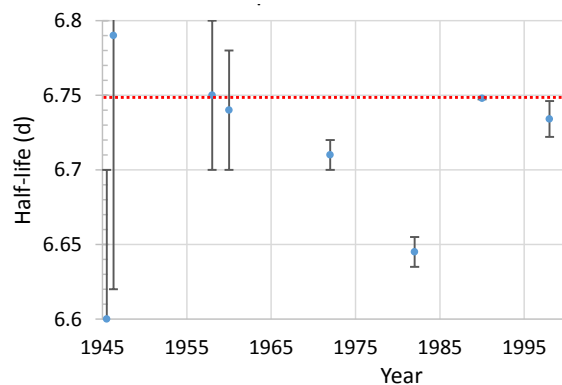
B.Q. Lee et al., Int J Radiat Biol 2016 & Radiother Oncol 2016;118 Suppl 1:S66.

Which nuclear data do we need for nuclear medicine?

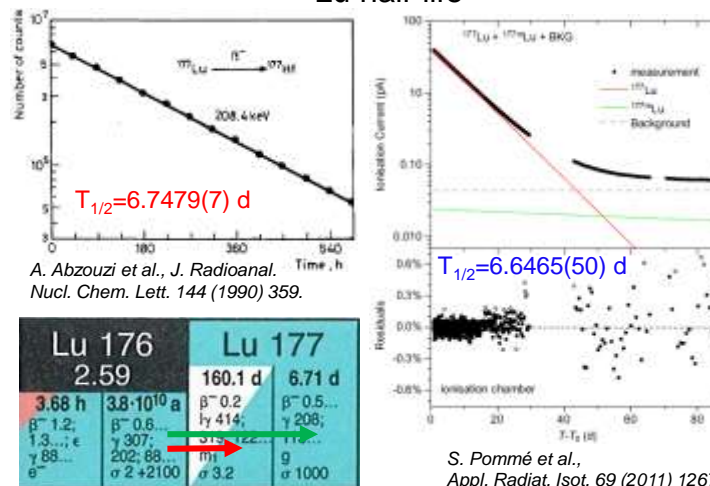
1. Half-life
2. Gamma ray energies (roughly!)
3. Particle spectra (electrons, alpha)
4. Cross-sections

Lu 176 2.6 σ 2100	Lu 177 6.7 d β^- 0.5... γ 208, 113... σ 1000
---------------------------------------	---

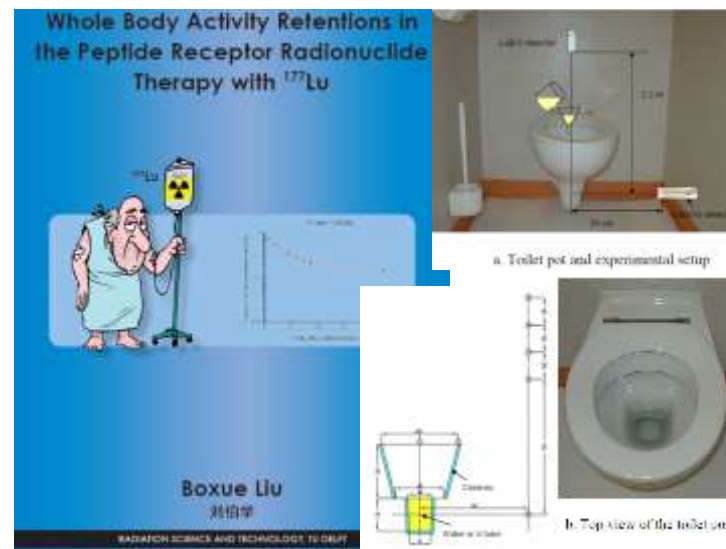
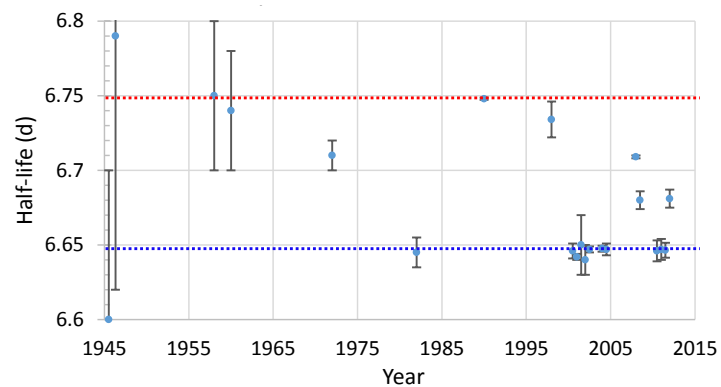
“Time dependence” of the ¹⁷⁷Lu half-life



¹⁷⁷Lu half-life



“Time dependence” of the ^{177}Lu half-life



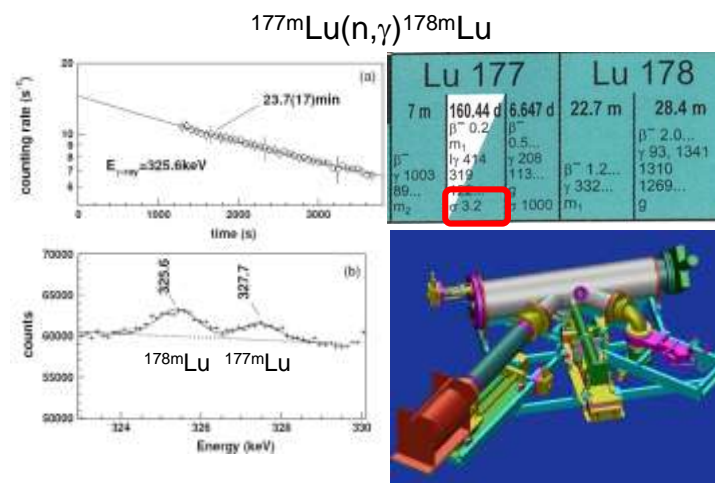
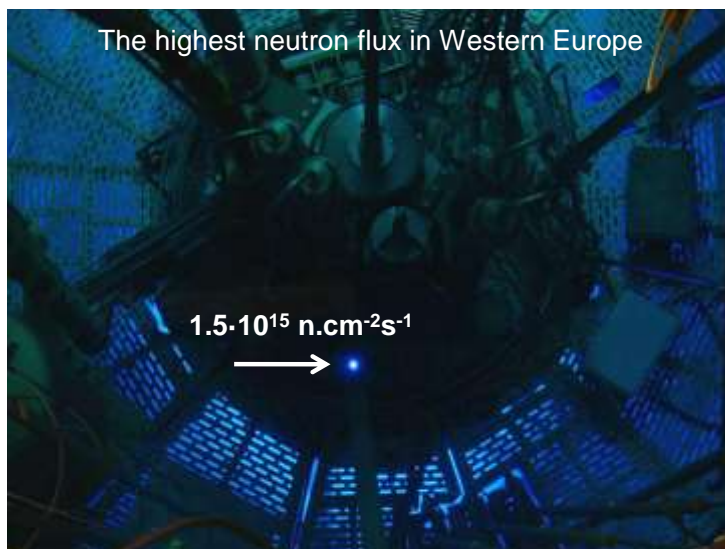
Bateman's nightmare – Phil Walker's dream



Thermal neutron capture cross-section σ_{th}
 Resonance integral I_γ
 In addition: Fast neutron cross-sections for (n,p), (n, α), (n,n')

$^{177m}\text{Lu}(n,\gamma)^{178m}\text{Lu}$

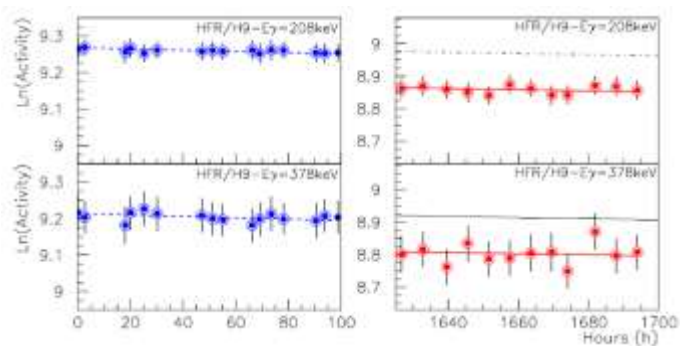
Lu 176		Lu 177		Lu 178	
2,599	7 m	160.44 d	6,647 d	22.7 m	28.4 m
β^- 1.2	β^- 0.6...	β^- 0.2	β^-	β^- 2.0...	β^- 2.0...
γ 113, 208...	γ 307, 202	γ 414	γ 208	γ 93, 1341	γ 93, 1341
σ 88...	σ 2 + 2100	σ 3.2	σ 1000	σ	σ



$\sigma[^{177\text{m}}\text{Lu}(n,\gamma)] = 368(26) \text{ b}$

G. Bélier et al.
Phys Rev C71, 014603 (2006)

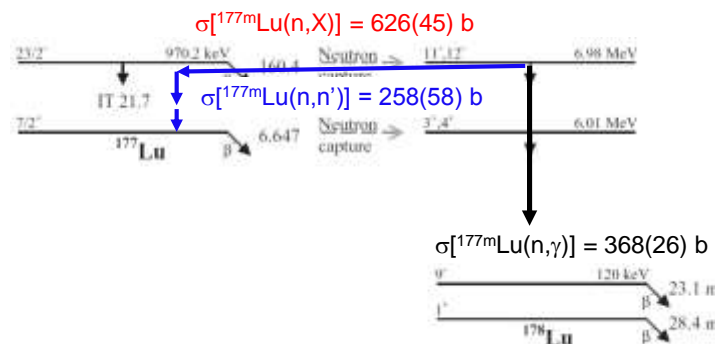
Measurement of burnup cross-section



$\sigma[^{177\text{m}}\text{Lu}(n,X)] = 626(45) \text{ b}$

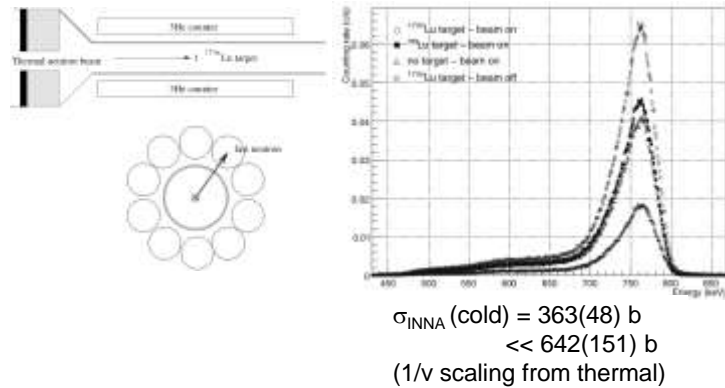
O. Roig et al. Phys Rev C71, 014603 (2006)

Inelastic neutron acceleration (INNA)



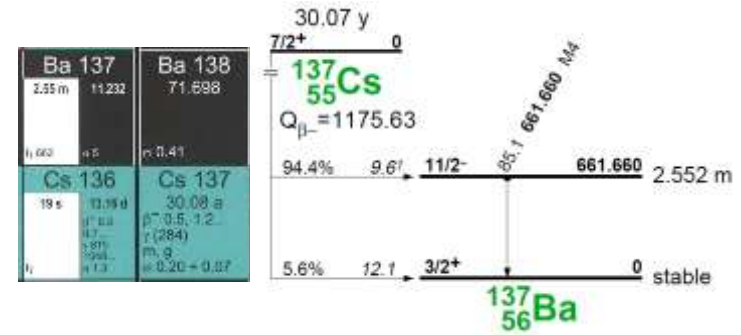
O. Roig et al. Phys Rev C71, 014603 (2006)

Direct observation of INNA



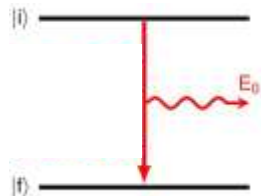
E. Bauge et al. Eur. Phys. J A48, 113 (2012)

Having fun with a nasty fission product: ^{137}Cs



The double-gamma decay

First discussed by Maria Göppert-Mayer in her doctoral thesis in 1930
 M. Göppert-Mayer, *Über Elementarakte mit zwei Quantensprüngen* (1930)



C Walz et al. Nature 526, 406 (2015)

The double-gamma decay

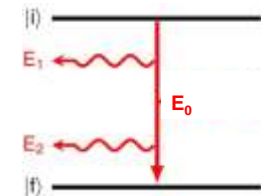
First discussed by Maria Göppert-Mayer in her doctoral thesis in 1930
 M. Göppert-Mayer, *Über Elementarakte mit zwei Quantensprüngen* (1930)



Second order process (10^{-6} weaker)

- $E_0 = E_1 + E_2$
- E_1, E_2 are continuous

well studied in atomic physics
 M. Lipes et al., PRL 15, 690 (1965)
 P.H. Mokler et al., Phys Scr 69, C1 (2004)
 K. Ilakovac et al., Rad Phys Chem 75, 1451 (2006)



Unit of 2-photon-absorption: $1 \text{ GM} = 10^{-50} \text{ cm}^4 \text{ s photon}^{-1}$

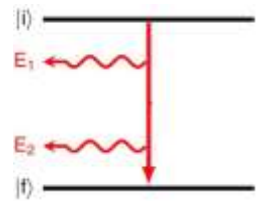
C Walz et al. Nature 526, 406 (2015)

The double-gamma decay in nuclear physics

$\gamma\gamma$ -decay only known in a special case:
 $0^+ \rightarrow 0^+$ (^{90}Zr , ^{40}Ca , ^{16}O)
 J. Schirmer et al., PRL 53, 1897 (1984)
 J. Kramp et al., NPA 474, 412 (1987)

never observed in competition to allowed single γ -transition
 W. Beusch et al., Helv Phys. Acta 33, 363 (1960)
 J. Kramp et al., NPA 474, 412 (1987)
 V.K. Basenko et al., Bull. Russ. Acad. 56, 94 (1992)
 C.J. Lister et al., Bull. Am. Phys. Soc. 58(13), DNP.CE.3 (2013)

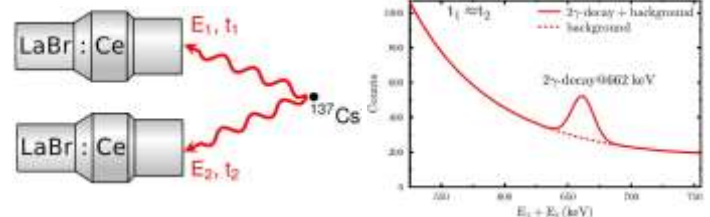
main experimental obstacle:
 presence of the one-photon decay



C Walz et al. Nature 526, 406 (2015)

Basic principle of the experiment

• use radioactive ^{137}Cs -source: 16.3(5) μCi

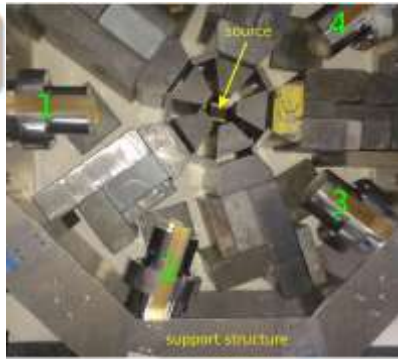


- background \leftrightarrow small decay probability (~1 event per day)
 - direct Compton scattering
 - random coincidences
 - cosmic rays, sequential Compton scattering, internal radioactivity

C Walz et al. Nature 526, 406 (2015)

The experimental setup & direct Compton scattering

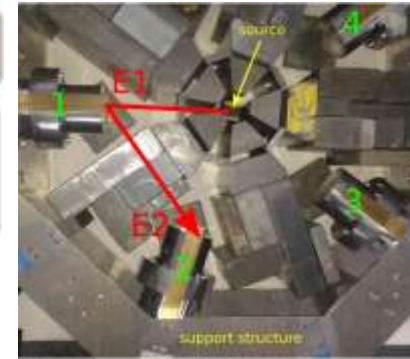
- 72°: 5 detector pairs
- 144°: 5 detector pairs



C Walz et al. Nature 526, 406 (2015)

The experimental setup & direct Compton scattering

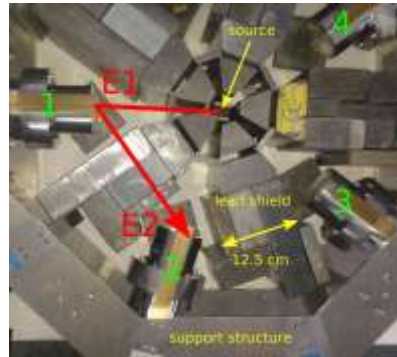
- 72°: 5 detector pairs
- 144°: 5 detector pairs
- $E_1 + E_2 = 662 \text{ keV}$
- Compton scattering \leftrightarrow double-gamma decay



C Walz et al. Nature 526, 406 (2015)

The experimental setup & direct Compton scattering

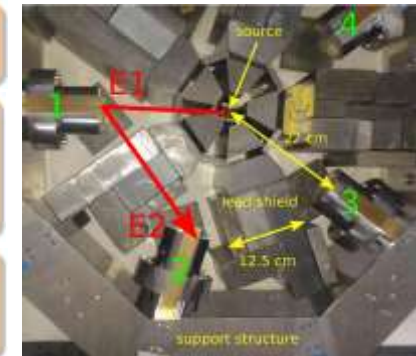
- 72°: 5 detector pairs
- 144°: 5 detector pairs
- $E_1 + E_2 = 662 \text{ keV}$
- Compton scattering \rightleftharpoons double-gamma decay



C Walz et al. Nature 526, 406 (2015)

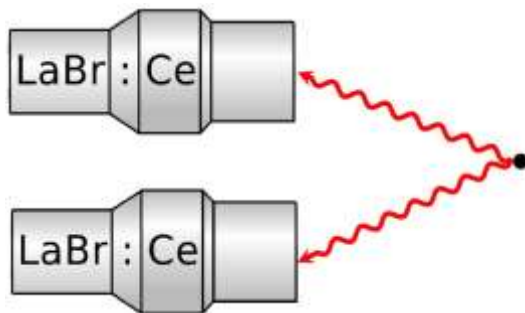
The experimental setup & direct Compton scattering

- 72°: 5 detector pairs
- 144°: 5 detector pairs
- $E_1 + E_2 = 662 \text{ keV}$
- Compton scattering \rightleftharpoons double-gamma decay
- $\epsilon_{\text{abs}} = 1.50(5)\%$
- measurement time: 1273 h



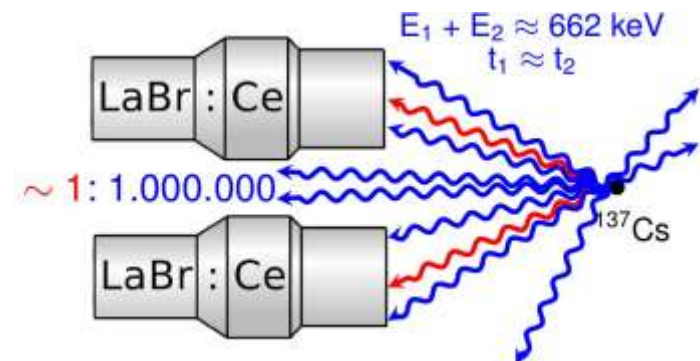
C Walz et al. Nature 526, 406 (2015)

Timing spectrum & random coincidences



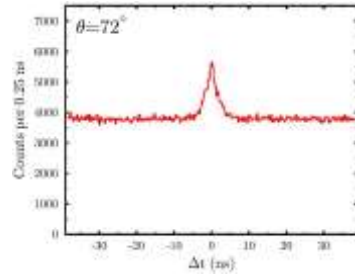
C Walz et al. Nature 526, 406 (2015)

Time spectrum & random coincidences



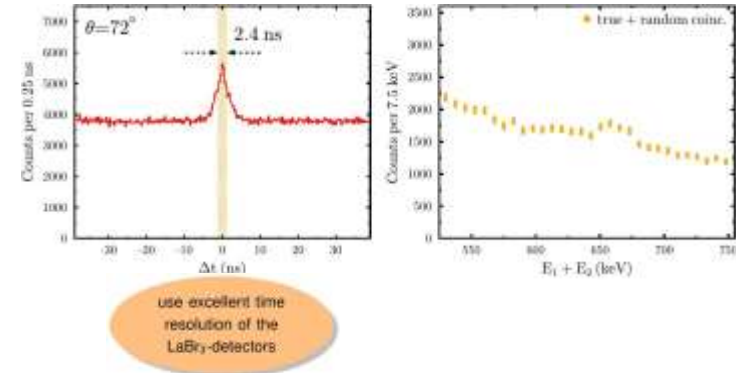
C Walz et al. Nature 526, 406 (2015)

Time spectrum & random coincidences



C Walz et al. Nature 526, 406 (2015)

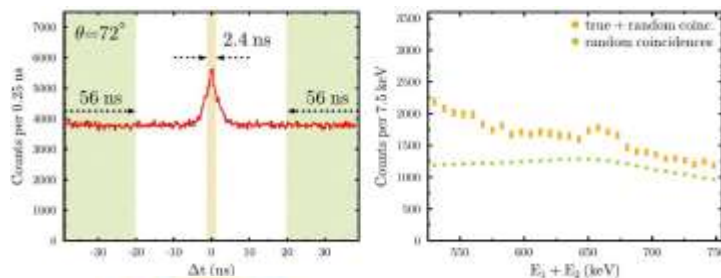
Time spectrum & random coincidences



use excellent time resolution of the LaBr3-detectors

C Walz et al. Nature 526, 406 (2015)

Time spectrum & random coincidences

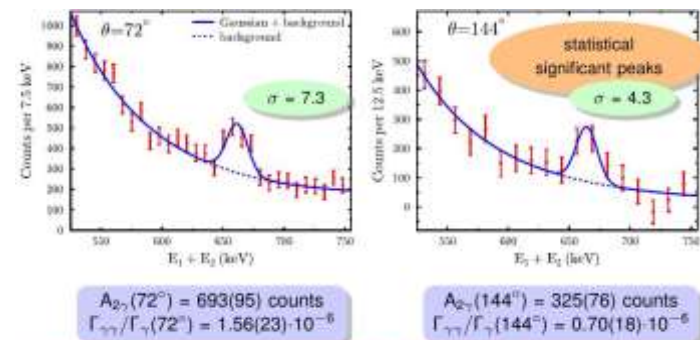


use excellent time resolution of the LaBr3-detectors

random coincidences determine uncertainty

C Walz et al. Nature 526, 406 (2015)

Results



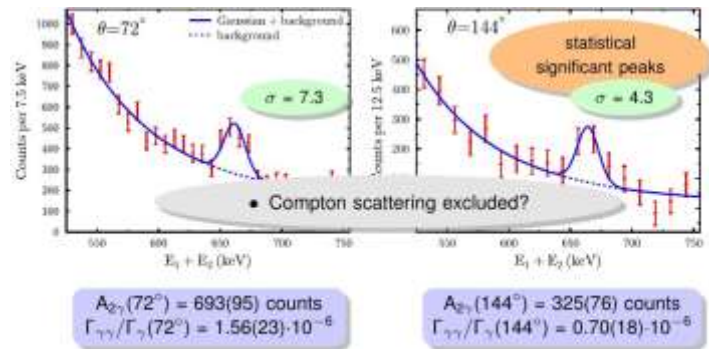
$A_{2\gamma}(72^\circ) = 693(95)$ counts
 $\Gamma_{2\gamma}/\Gamma_\gamma(72^\circ) = 1.56(23) \cdot 10^{-6}$

$A_{2\gamma}(144^\circ) = 325(76)$ counts
 $\Gamma_{2\gamma}/\Gamma_\gamma(144^\circ) = 0.70(18) \cdot 10^{-6}$

Result: Successful observation of the competitive double-gamma decay

C Walz et al. Nature 526, 406 (2015)

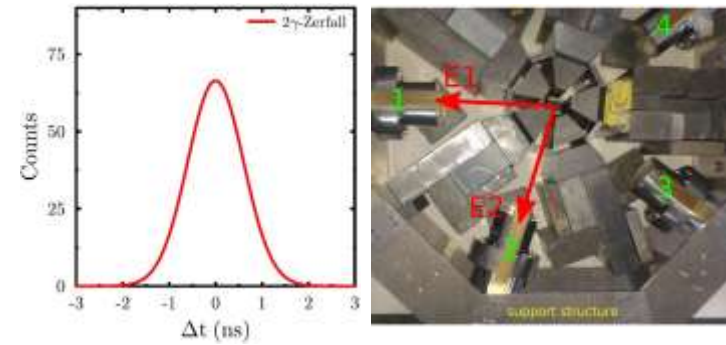
Results



► Result: Successful observation of the competitive double-gamma decay

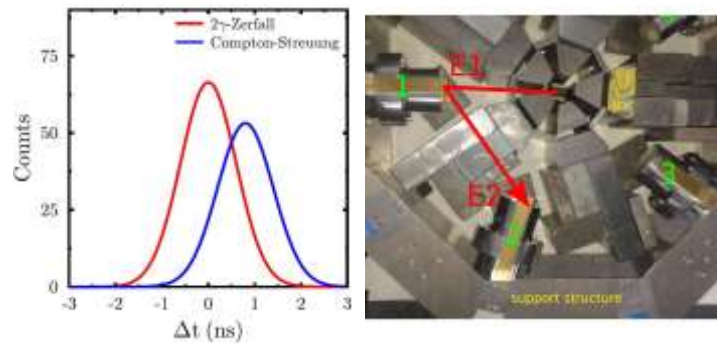
C Walz et al. Nature 526, 406 (2015)

Critical analysis (1)



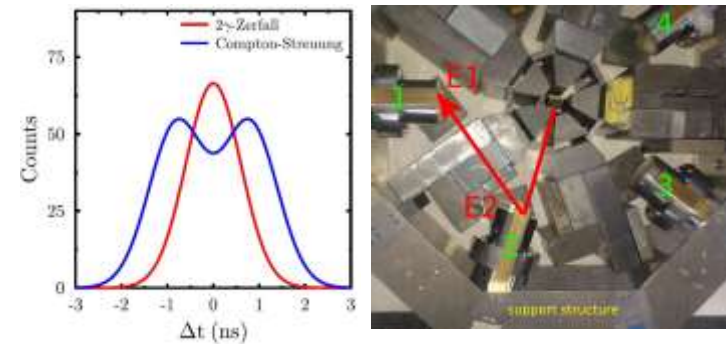
C Walz et al. Nature 526, 406 (2015)

Critical analysis (1)



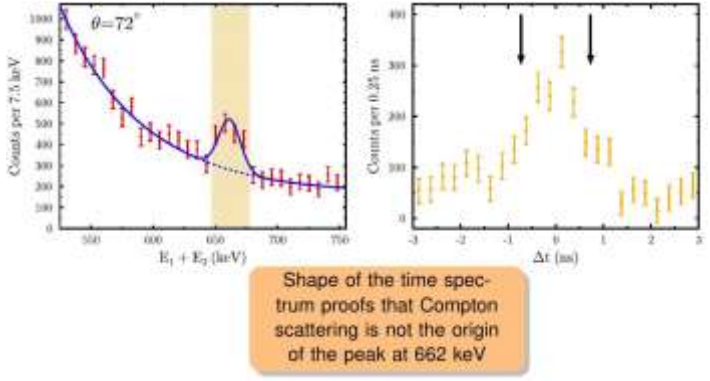
C Walz et al. Nature 526, 406 (2015)

Critical analysis (1)



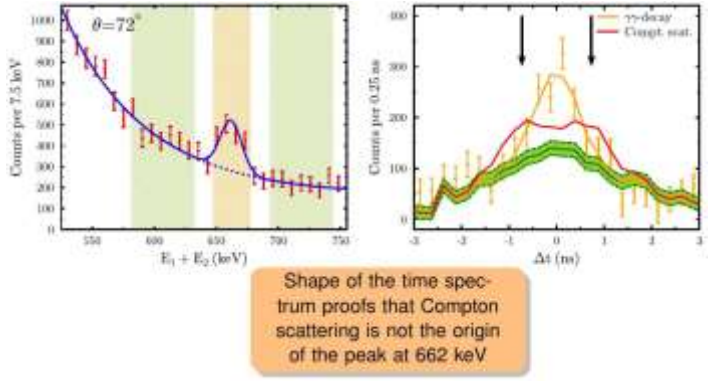
C Walz et al. Nature 526, 406 (2015)

Critical analysis (2)



C Walz et al. Nature 526, 406 (2015)

Critical analysis (2)

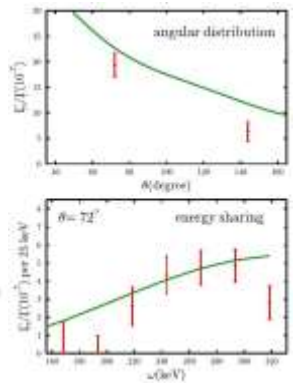


C Walz et al. Nature 526, 406 (2015)

Results & comparison to QPM

	exp	QPM
$\Gamma_{\gamma\gamma}/\Gamma_{\gamma}(10^{-8})$	2.1(3)	2.69
$\alpha_{M2E2}(\frac{e^2 \text{fm}^4}{\text{MeV}^2})$	+38.2(36)	+42.6
$\alpha_{E3M1}(\frac{e^2 \text{fm}^4}{\text{MeV}^2})$	+7.4(38)	+9.5

- ▶ α_{M2E2} dominates
- ▶ relative sign between α_{M2E2} and α_{E3M1} is positive
- ▶ good description in the framework of the QPM



C Walz et al. Nature 526, 406 (2015)

Dependence of radioactive decay on external conditions?

The nuclear decay constant is a fundamental constant which cannot be changed by external, non-nuclear processes.

E Rutherford and F Soddy, J Chem Soc Trans 81, 837 (1902)

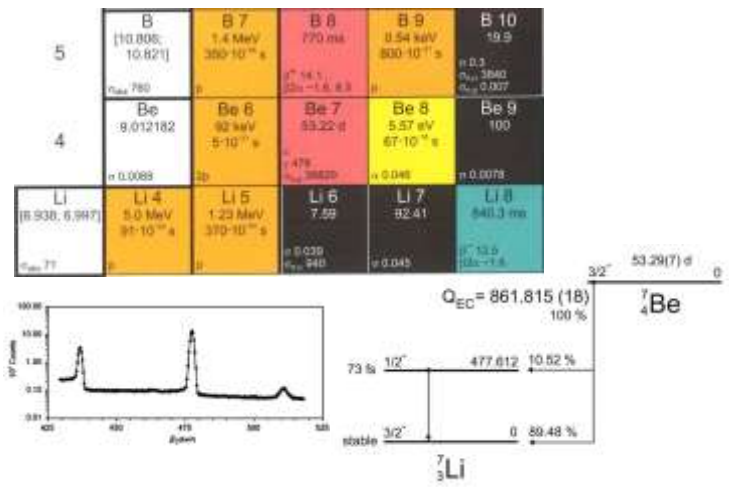
Effects of temperature, pressure, electromagnetic fields, chemistry, etc. less than 1%.

GT Emery, Ann Rev Nucl Sci 22, 165 (1972)

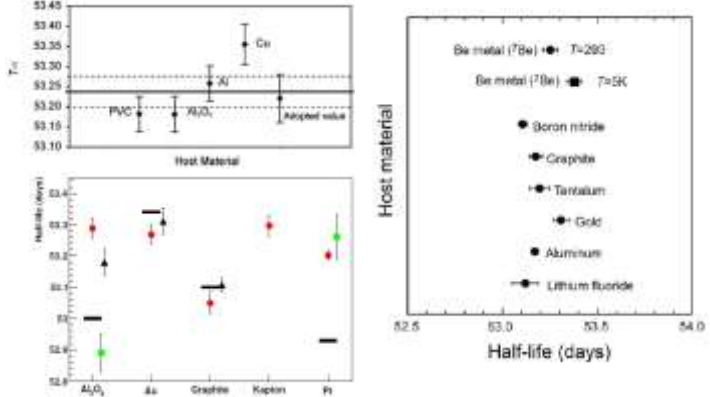
No dependence on season, moon phase, government, etc.

However,

⁷Be: the lightest EC decaying isotope

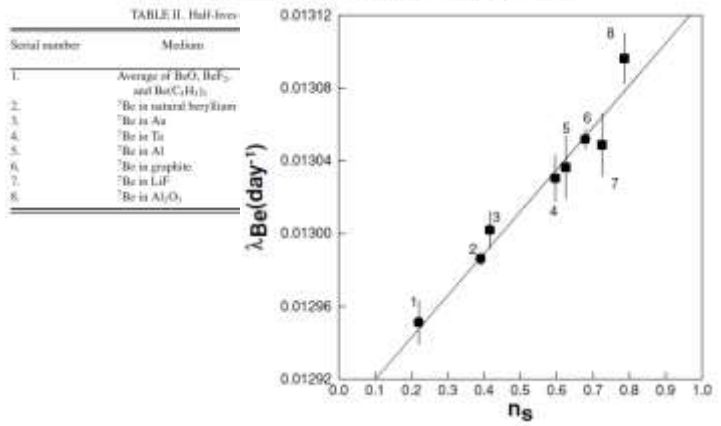


Different implantation conditions



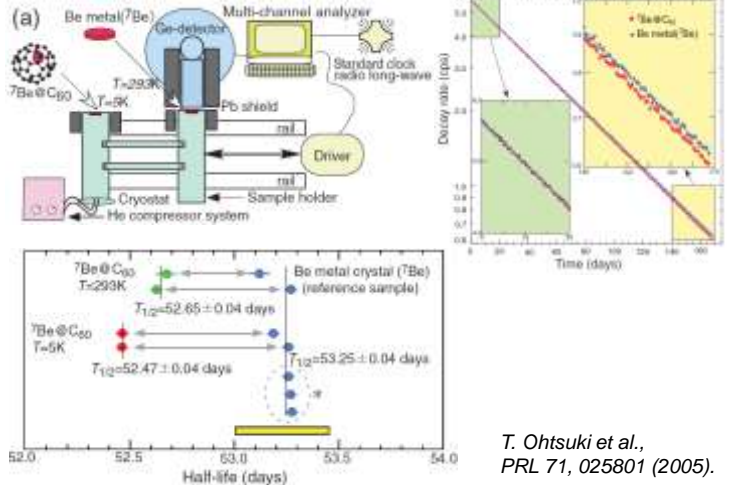
Y. Nir-El et al., *Phys Rev C* 75, 012801 (2012).
 C. Mazzocchi et al., *Acta Phys Pol B* 43, 279 (2012).
 T. Ohtsuki et al., *Proc Radiochim Acta* 1, 101 (2011).

Systematics of ⁷Be decay rate measurements



P. Das and A. Ray, *Phys Rev C* 71, 025801 (2005).

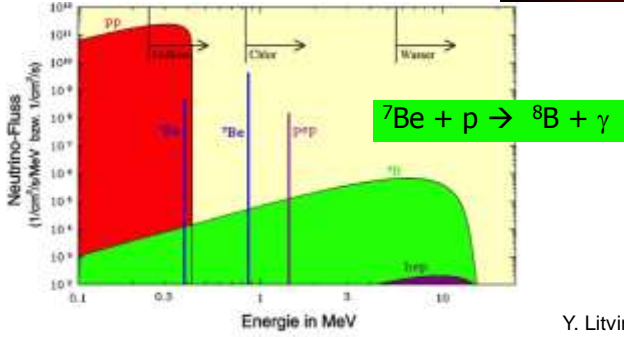
1.5% record change of half-life in cooled fullerenes



T. Ohtsuki et al., *PRL* 71, 025801 (2005).

⁷Be decay in the Sun

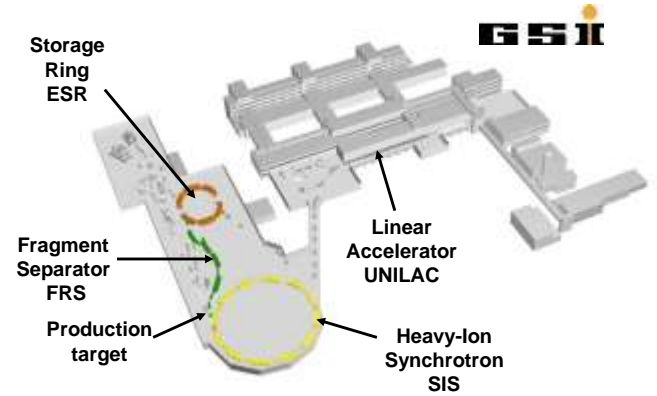
Ionization of ⁷Be in the Sun can be ~20-30 %
 AV Gruzinov, JN Bahcall, Astroph J 490, 437 (1997)



Y. Litvinov, GSI

Change the electron density more radically ?

⇒ highly charged ions



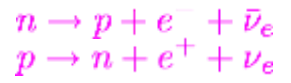
Y. Litvinov, GSI

Nuclear beta decay

Nuclear weak decay in general form:

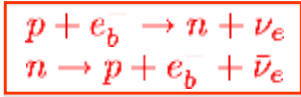


i) continuum beta decay:



β^- - decay
 β^+ - decay

ii) two-body beta decay:



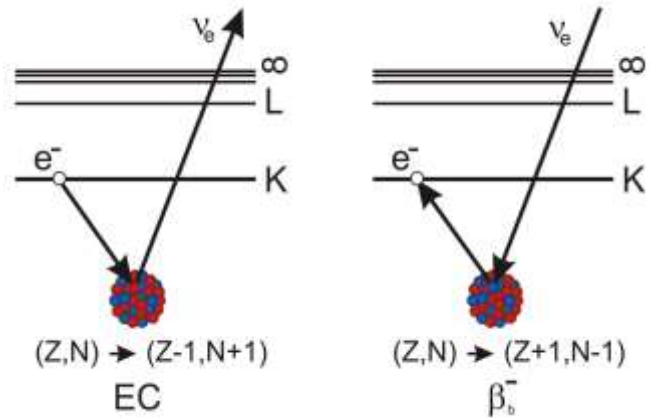
Orbital electron capture (EC)
 Bound state beta decay (β_b^-)



Free electron capture

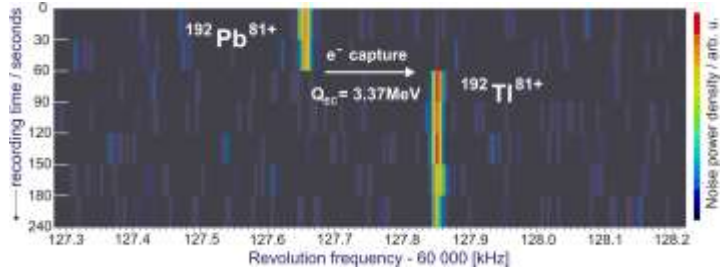
Y. Litvinov, GSI

Two-body beta decay



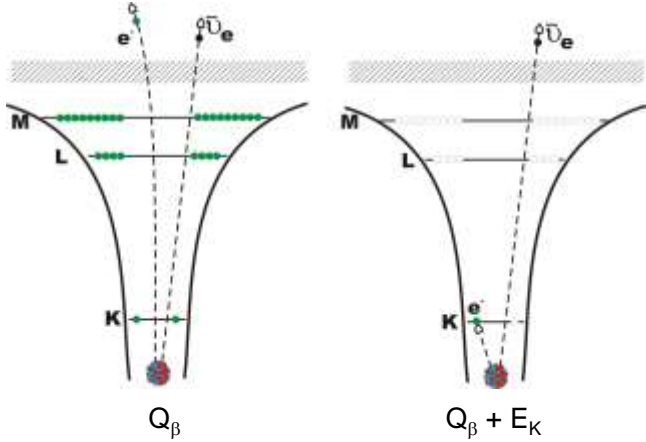
Y. Litvinov, GSI

Observation in Schottky frequency spectra



Y. Litvinov, GSI

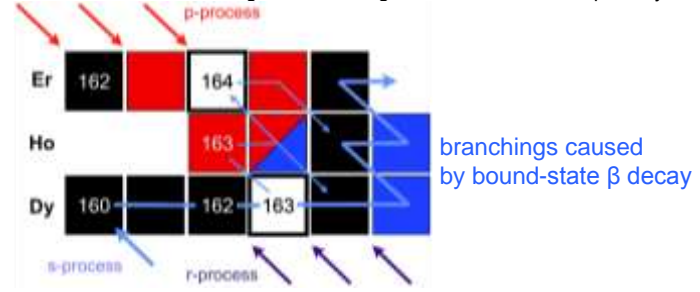
Bound-state beta decay



Y. Litvinov, GSI

Bound state beta decay of ¹⁶³Dy

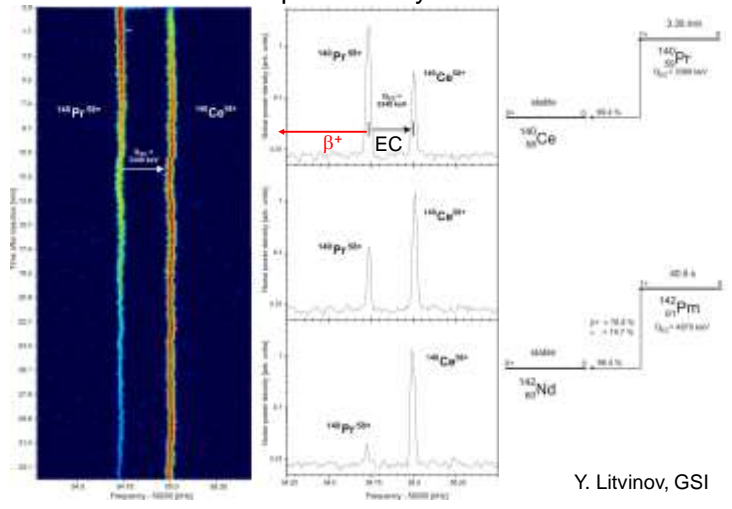
s process: slow neutron capture and β⁻ decay near valley of β stability at kT = 30 keV; → high atomic charge state → bound-state β decay



¹⁶³Dy $Q_\beta = -2.8 \text{ keV}$ stable
¹⁶³Dy⁶⁶⁺ $Q_\beta + E_K = +50 \text{ keV}$ $T_{1/2} = 47(5) \text{ d}$
 (L capture also energetically allowed but negligible due to Q^5)

M. Jung et al., Phys. Rev. Lett. 69 (1992) 2164 Y. Litvinov, GSI

Orbital electron capture decay of few-electron ions



Y. Litvinov, GSI

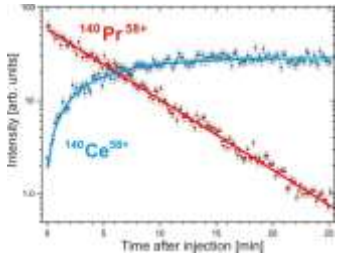
Orbital electron capture decay of few-electron ions

Expectations:

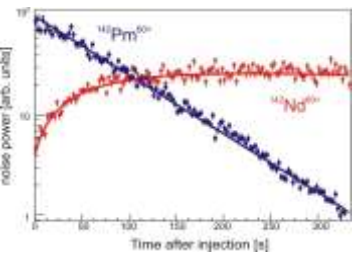
$$\lambda_{EC}(\text{H-like}) / \lambda_{EC}(\text{He-like}) \approx 0.5$$

$$\lambda_{EC}(\text{H-like}) / \lambda_{EC}(\text{He-like}) = 1.49(8)$$

$$\lambda_{EC}(\text{H-like}) / \lambda_{EC}(\text{He-like}) = 1.44(6)$$



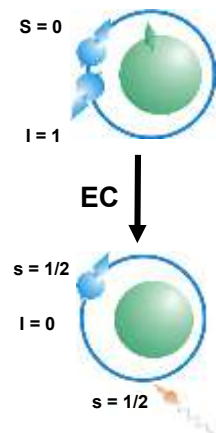
Yu.A. Litvinov et al., Phys. Rev. Lett. 99 (2007) 262501



N. Winckler et al., Phys. Lett. B579 (2009) 36

Y. Litvinov, GSI

Selection rule



$F = 1$

$$\lambda_{EC}^{\text{H}} = \lambda_{EC}^{\text{He}} \cdot \frac{2I_i + 1}{2F_i + 1}$$

$$I_i = 1$$

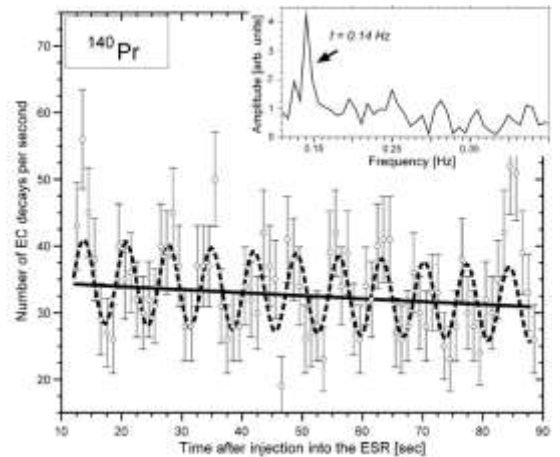
$$F_i = I_i - s = 1/2$$

$$F_i = I_i + s = 3/2$$

$F = 1$

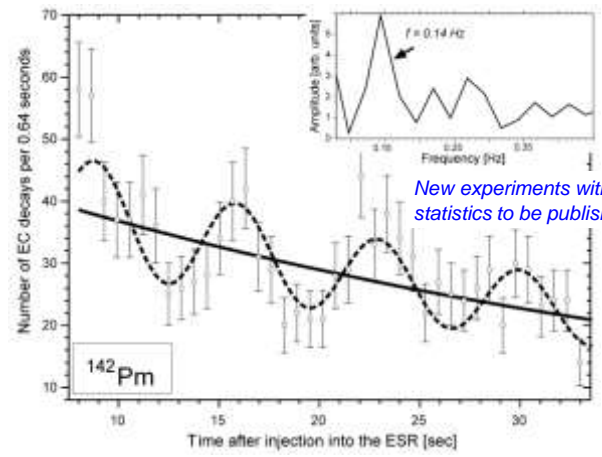
Y. Litvinov, GSI

Non-exponential decay: the "GSI anomaly"



Y. Litvinov et al., Phys. Lett. B664 (2008) 162

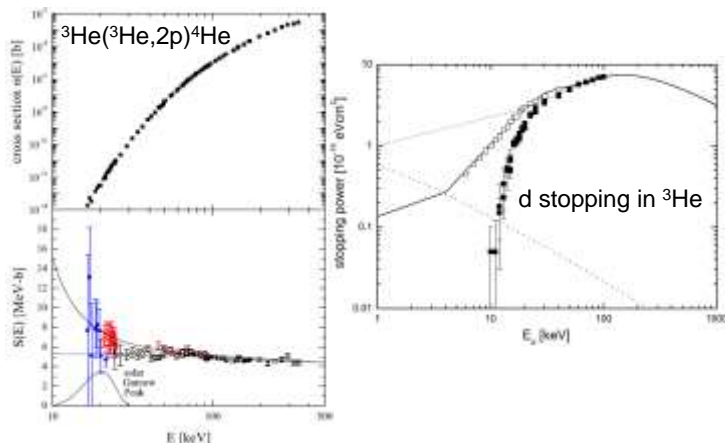
Non-exponential decay: the "GSI anomaly"



New experiments with high statistics to be published...

Y. Litvinov et al., Phys. Lett. B664 (2008) 162

Nuclear astrophysics: fusion well below Coulomb barrier



H. Costantini et al., Rep Prog Phys 72, 086301 (2009)

Electron screening in low-energy fusion reactions

cross-sections below Coulomb barrier significantly enhanced by electron screening:

$$f_{\text{lab}}(E) = E(E + U_e)^{-1} \exp(\pi\eta U_e/E)$$

U_e screening energy ≈ 300 eV for d(d,p)t reaction when deuterium is embedded in metals

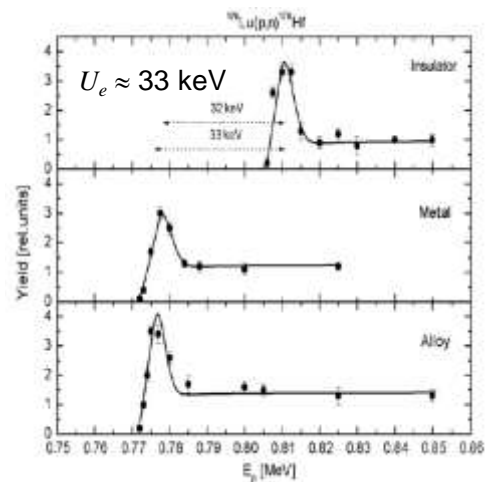
U_e screening energy $\approx U_D$ from Debye model should scale with nuclear charge of target.

$$U_D = 2.09 \times 10^{-11} (Z_1(Z_1 + 1))^{1/2} (n_{\text{eff}} \rho_A / T)^{1/2} \text{ (eV)}$$

$U_D = 21(6)$ keV predicted for Lu and $36(4)$ keV for PdLu_{0.1} alloy

K.U. Kettner et al., J Phys G 32, 489 (2006)

Electron screening in low-energy fusion reactions



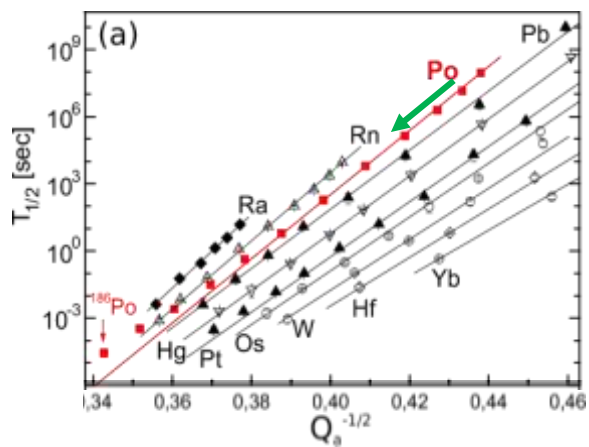
K.U. Kettner et al., J Phys G 32, 489 (2006)

Proposed scaling to low temperatures

One major reason of the present work, i.e. to extend screening tests up to $Z_1 = 71$, was another prediction of the Debye model concerning radioactive decay of transuranic nuclides ($Z_1 \geq 82$) in a metallic environment [5]. In general, for the α -decay and β^- -decay one expects a shorter half-life due to the acceleration mechanism of the Debye electrons for these positively charged particles similar as for the protons, deuterons or ${}^3\text{He}$ in the fusion reactions, while for the β^- -decay and e-capture process one predicts a longer half-life (here, deceleration for the negatively charged particles). For example, if the α -decay ${}^{210}\text{Po} \rightarrow \alpha + {}^{206}\text{Pb}$ with $E_\alpha = 5.30$ MeV and $T_{1/2} = 138$ days occurs in a metal cooled to $T = 4$ K, one arrives at $U_D = Z_1 Z_2 U_e (d+d) (290/4)^{1/2} = 2 \times 82 \times 300 \text{ eV} \times 8.5 = 420$ keV, where we used again a typical value of $U_e = 300$ eV for the d+d fusion reaction in metals at $T = 290$ K. The enhancement factor then gives $f_{\text{lab}} = 265$, and thus the half-life is shortened to 0.5 days. For the biologically dangerous transuranic waste [12] ${}^{226}\text{Ra} \rightarrow \alpha + {}^{222}\text{Rn}$ ($E_\alpha = 4.78$ MeV, $T_{1/2} = 1600$ years) an analogous calculation leads to $T_{1/2} = 1.3$ years. Experiments are in progress to test these predictions: If these predictions of the Debye model should also be verified, one may have a cheap solution to remove the transuranic waste (involving all an α -decay) of used-up rods of fission reactors in a time period of a few years. Finally, a reduced half-life of α -emitters such

K.U. Kettner et al., J Phys G 32, 489 (2006)

Geiger Nuttall rule for alpha-decay

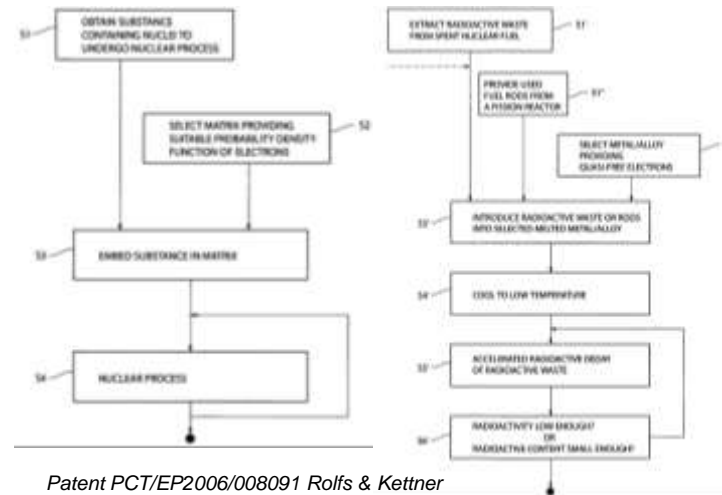


C. Qi et al. Phys.Lett. B734 (2014) 203.

Experiments invalidate application of Debye model !

- ^{22}Na in Pd at 12 K: 1.2(2)% faster β^+ decay vs. 11% predicted
B Limata et al., Eur Phys J A 28, 251 (2006)
- ^{210}Po in Cu at 12 K: 6.3(14)% faster α decay vs. 1000% predicted
F Raiola et al., Eur Phys J A (2007)
- ^{253}Es in Fe at 4 K: 0.4(3)% faster α decay vs. 10^2 predicted
- ^{253}Es in Fe at 50 mK: 1.4(6)% faster α decay vs. $\gg 10^6$ predicted
N Severijns et al., Phys Rev C 76, 024304 (2007)
- ^{224}Ra in Fe, at 1 K and 20 mK: <1% effect on $T_{1/2}$
- ^{225}Ra in Fe, at 1 K and 20 mK: <0.5% effect on $T_{1/2}$
- ^{227}Ac in Fe, at 1 K and 20 mK: <1% effect on $T_{1/2}$
vs. effects of 10^4 to 10^{10} predicted by Debye model
NJ Stone et al., Nucl Phys A 793, 1 (2007)

“Cool” solution for nuclear waste ?



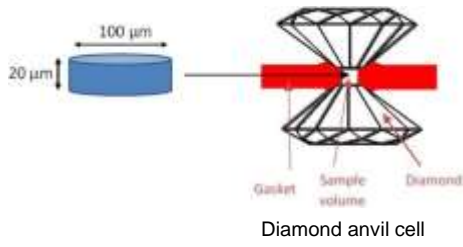
Patent PCT/EP2006/008091 Rolfs & Kettner

Theoretical arguments

Correct treatment of screening effects in tunnelling of alpha particles gives for ^{210}Po and ^{226}Ra at 4 K a predicted **half-life increase of <0.1%** with the Debye model and 0.9% and 1.3% with the Thomas-Fermi model.

N.T. Zinner, Nucl. Phys. A 781, 81 (2007)

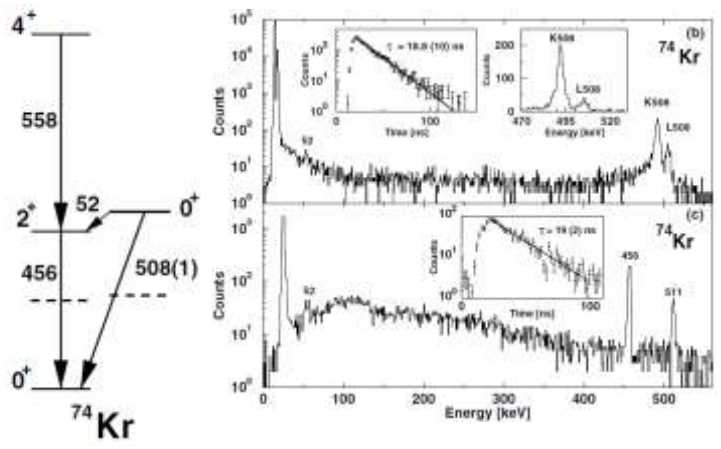
Effect of pressure on alpha decay ?



Expected effect: -0.02% half-life change for ²⁴¹Am at 0.5 MBar

N. Nissim et al. PRC 94, 014601 (2016)

Isomeric decay

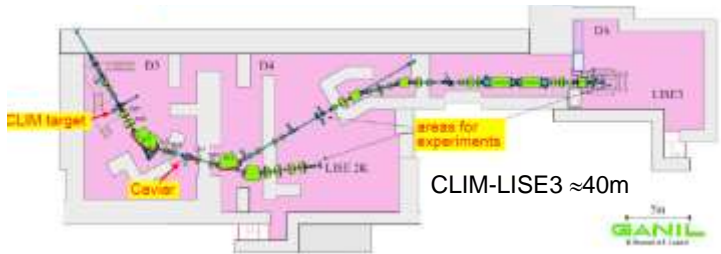


E. Bouchez et al. PRL 90, 082502 (2003)

Decay losses in flight ?

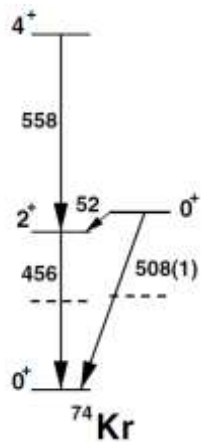
TOF \approx 400 ns
 $\tau = 18.8$ ns, i.e. $T_{1/2} = 13.0$ ns

$\exp(-400/18.8) \approx 6 \cdot 10^{-10}$



R. Anne et al., Nucl. Instr. Meth. A257 (1987) 215.
 R. Anne et al., Nucl. Instr. Meth. B70 (1992) 276.

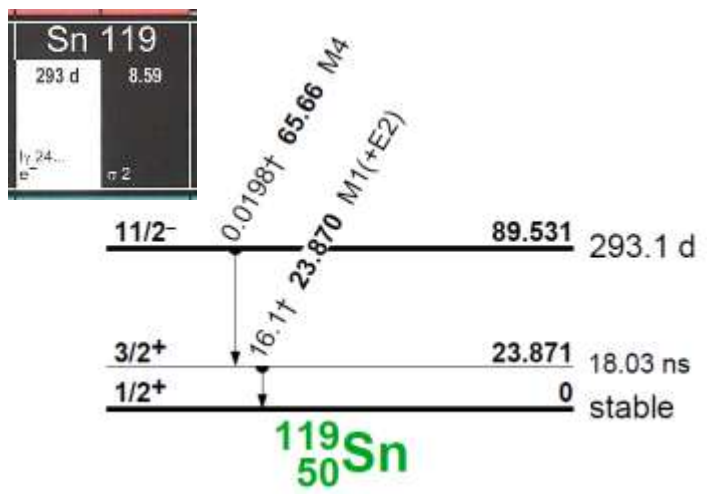
Isomeric decay of fully stripped ⁷⁴Kr³⁶⁺



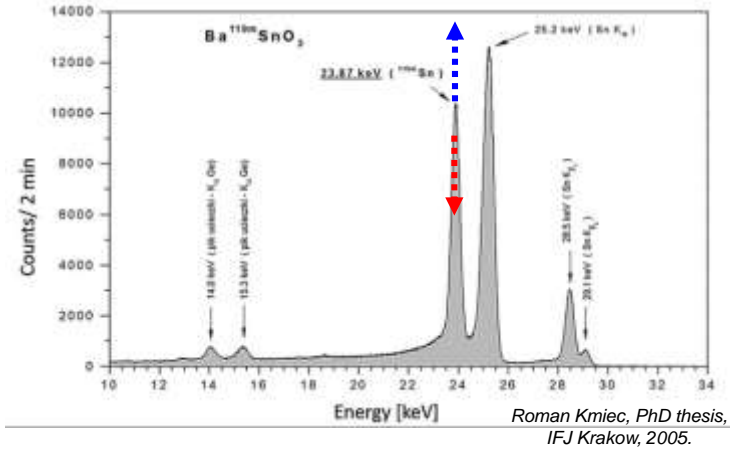
$\tau = 18.8$ ns = $1/\lambda(E2) + 1/\lambda(E0)$
 $\lambda(E2) / \lambda(E0) = 1.2$
 $\tau(E2) = 34.4$ ns ~~$\tau(E0) = 41.5$ ns~~
 $\alpha(E2) = 8.7 = [\text{decays by CE}] / [\text{all decays}]$
 $\tau(E2-\gamma) = (\alpha(E2)+1) \cdot \tau(E2) = 334$ ns
 $\exp(-400/334) = 0.3$

E. Bouchez et al. PRL 90, 082502 (2003)

Isomeric decay of ^{119m}Sn

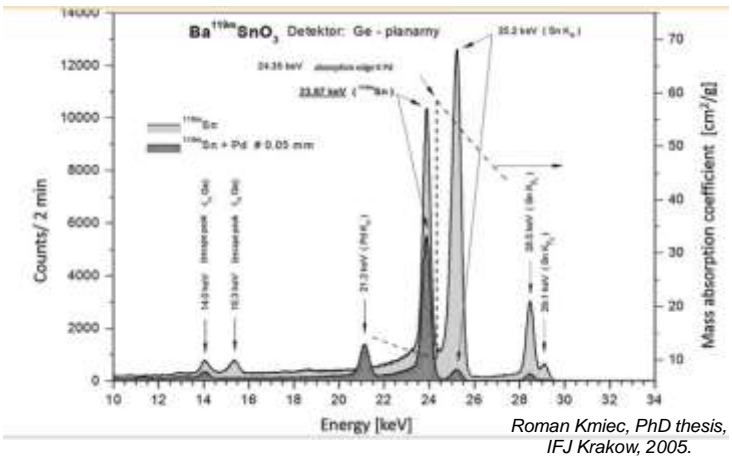


^{119m}Sn spectrum with planar Ge detector



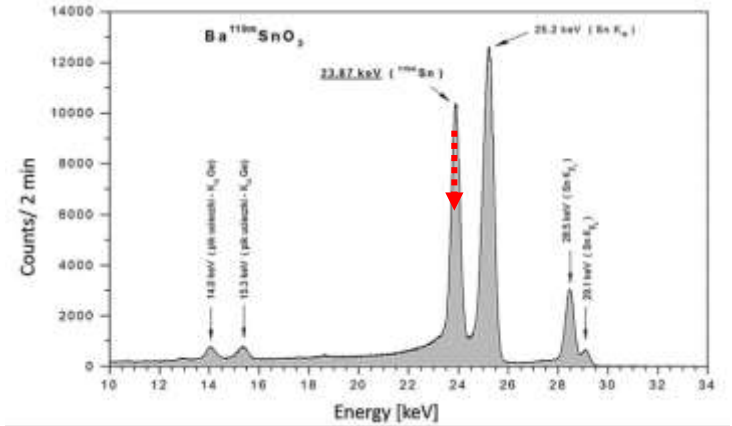
Roman Kmiec, PhD thesis, IFJ Krakow, 2005.

Attenuation with Pd layer



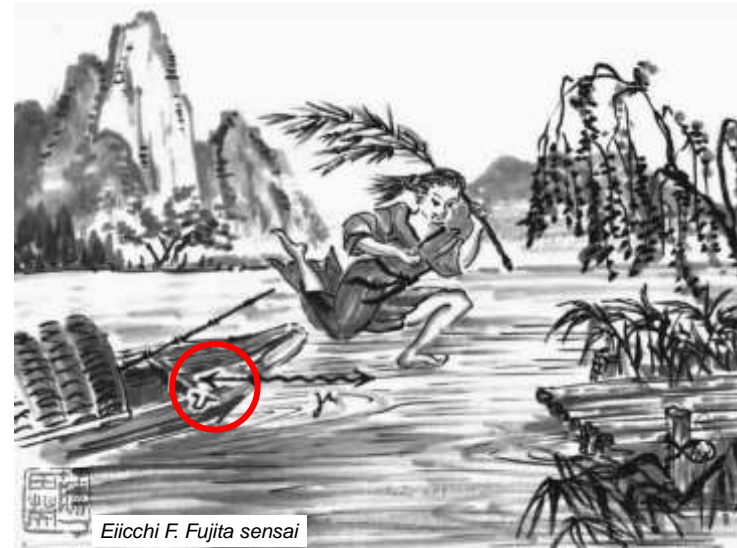
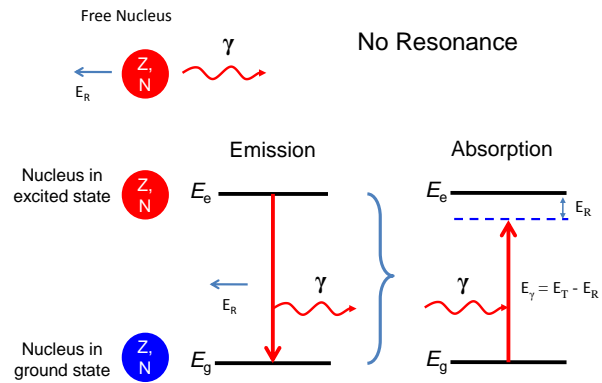
Roman Kmiec, PhD thesis, IFJ Krakow, 2005.

Attenuation with Sn layer

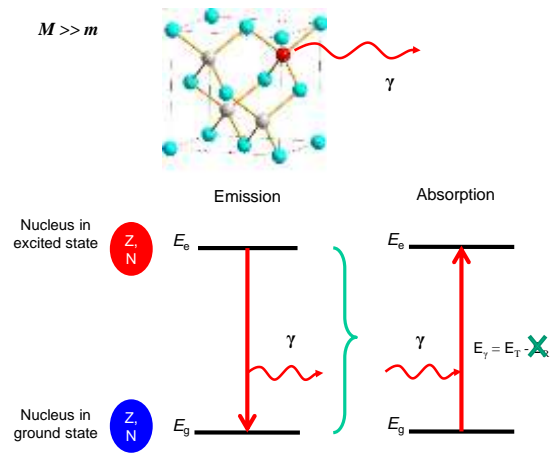


Resonant nuclear attenuation $\approx 1000 \cdot$ non-resonant attenuation

Nuclear resonance fluorescence



Recoilless nuclear resonance fluorescence



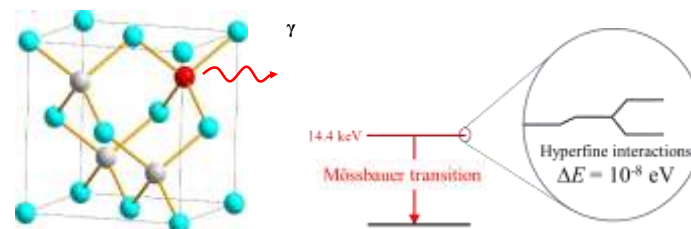
Mössbauer effect

1957 discovery of recoilless nuclear resonance
 1961 Nobel Prize in Physics



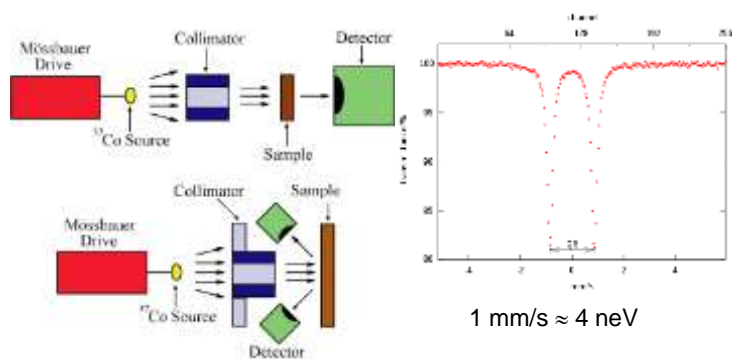
Application of the Mössbauer effect

Interactions between the nucleus and its surrounding electrons...



...causing changes in the nuclear (and electronic) energy levels.

Mössbauer spectroscopy

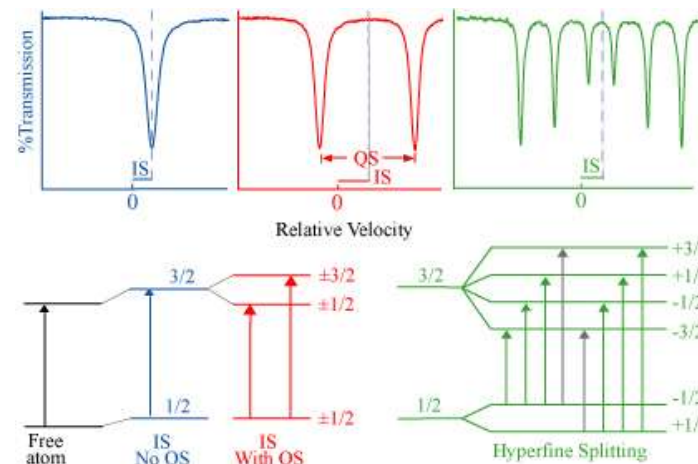


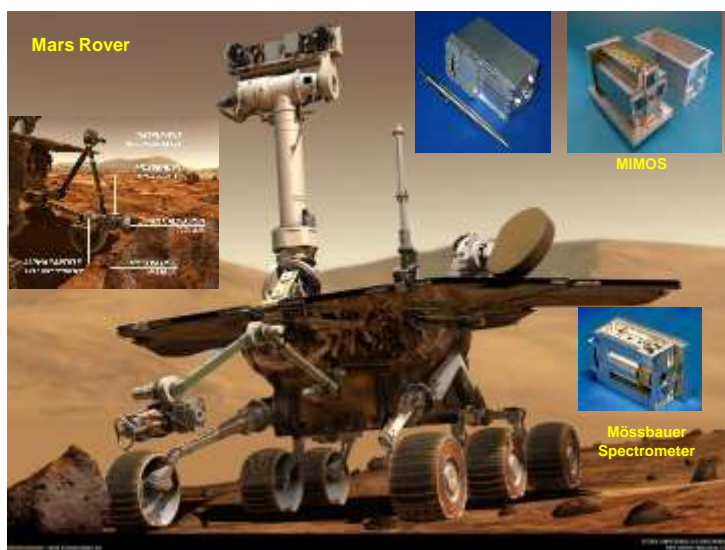
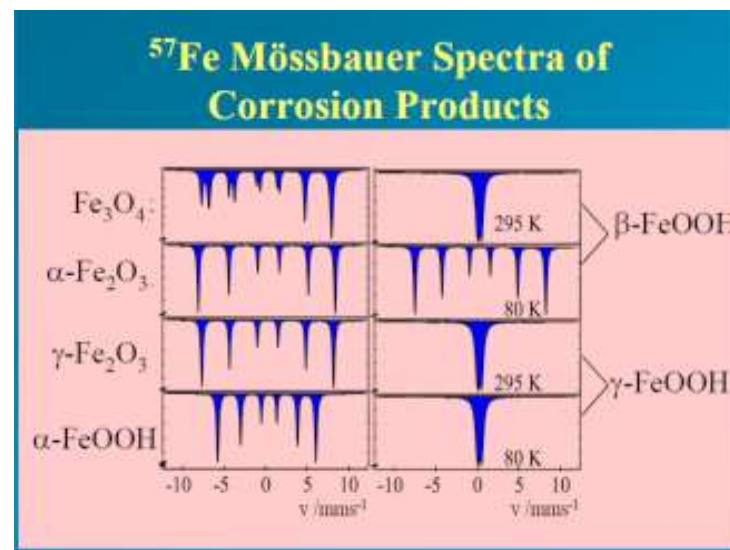
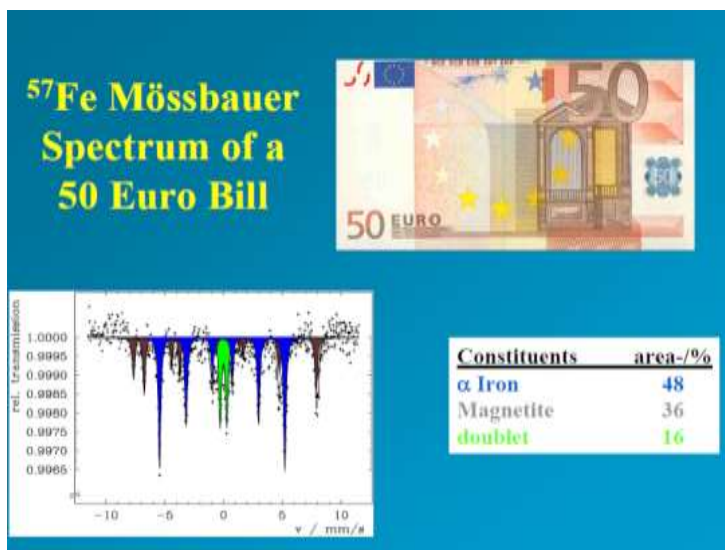
$$\Delta E = \hbar/\tau$$

$$^{57}\text{Fe}: \tau = 140 \text{ ns} \Rightarrow \Delta E = 5 \text{ neV}$$

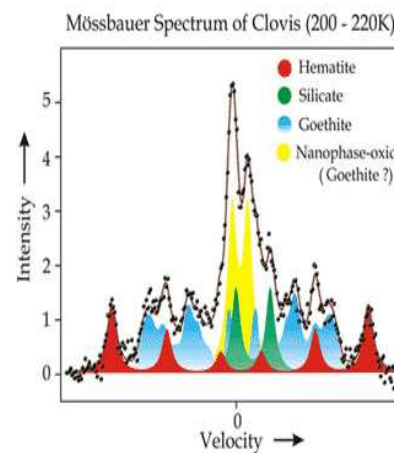
$$\Delta E/E = 3 \cdot 10^{-13}$$

Hyperfine interactions



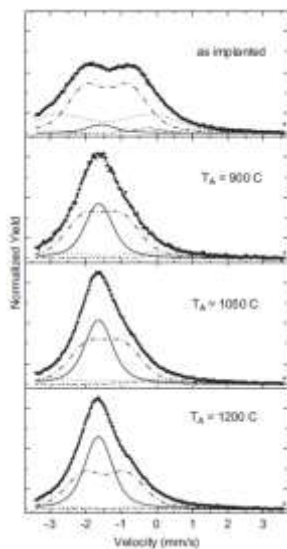


Nuclear method proofs water was on Mars

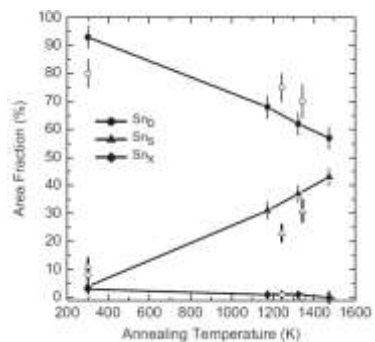


Goethite contains hydroxyl (OH^-) as a part of its structure.

\rightarrow water



^{119m}Sn implanted into diamond



K Bharut-Ram et al. Physica B 407, 2923 (2012)

Summary

Physics close to stability remains exciting !

Very high resolution and/or sensitivity and good control of systematics are essential to study subtle effects.

New, astonishing effects may either indicate new physics, or they will disappear with better statistics and/or higher resolution.

Develop your own judgement !

Acknowledgements

Thanks for useful slides and input from:

Roger Brissot (LPSC Grenoble), Olivier Serot (CEA Cadarache), Boon Quan Lee (ANU Canberra), Norbert Pietralla (TU Darmstadt), Yuri Litvinov (GSI Darmstadt), Palle Gunnlaugsson (KU Leuven) and Philipp Gütlich (Univ. Mainz).